

Franz-Peter Reiter

**Functionalised monolithic separation media derived
by ring-opening metathesis polymerisation:
Applicability in capillary ion-exchange-HPLC**

DIPLOMA THESIS

for obtaining the degree of a graduate engineer in
Technical Chemistry

Graz, University of Technology

in collaboration with the Institute of Medical
Technologies and Health Management,
JOANNEUM RESEARCH, Graz

Personal tutor Univ.-Prof. Dipl.-Ing. Dr. techn. Ernst Lankmayr,
Institute of Analytical Chemistry and Radiochemistry,

June 2007 – April 2008

Abstract

Over the past years monolithic separation media became an often used way to meet the high -and still increasing- standards of biotechnology and medicine in analytical methods. The main advantages of these media are their low back pressure, fast mass transfer and the easy possibility for miniaturisation because of the elimination of packing procedures. Previous investigations already showed that ring-opening metathesis polymerisation (ROMP) is an efficient approach to such monolithic media. To broaden the fields of the applicability of miniaturised monolithic columns, investigations of regarding their surface modification have been done, but the chromatographic properties of the resulting separation media have haven't been studied so far.

Therefore, the objective for the present work was the characterisation of functional, miniaturised monolithic separation media for cap-HPLC prepared via ROMP. Monolithic columns with 200µm inner diameter for cation-exchange (CX) and anion-exchange (AX) chromatography have been investigated. The influence of functionalisation techniques as well as different functionalisation parameter on the chromatographic properties has been evaluated with the separation of a peptide standard for CX-columns and an oligonucleotide standard for AX-columns. The investigated media showed in general good separation performance and a clear influence of the functionalisation parameter on it. Closing, the clinical applicability of these media was investigated; a method for the online-solid phase extraction of imiquimod in human biofluids which shows good results was developed.

Zusammenfassung

In den letzten Jahren wurden monolithische Trennmedien immer öfter eingesetzt um die hohen und noch immer weiter steigenden Anforderungen an analytischen Methoden in der Biotechnologie und der Medizin zu erfüllen. Die großen Vorteile von monolithischen Medien sind ihr geringer Gegendruck, der schnelle Massentransfer und der einfache Zugang miniaturisierten Trennmedien durch den nicht vorhandenen Packungsvorgang im Vergleich zu partikulären Materialien. Frühere Studien zeigten bereits, dass die ringöffnende Metathese Polymerisation (ROMP) einen effizienten Weg zu monolithischen Trennmedien bietet; auch die Miniaturisierung dieser Medien wurde bereits gezeigt. Um das Anwendungsspektrum miniaturisierter monolithischer Materialien weiter zu vergrößern, wurden bereits Versuche zur Oberflächenmodifikation durchgeführt, die chromatographischen Eigenschaften der resultierenden Trennmedien wurden allerdings noch nicht genauer untersucht.

Die Hauptaufgabe der vorliegenden Arbeit war somit die Charakterisierung von mittels ROMP hergestellter, funktionalisierter, miniaturisierter stationärer Phasen für den Einsatz in der cap-HPLC. Monolithische Trennsäulen von 200µm Innendurchmesser für Kationen- und Anionenaustauschchromatographie wurden untersucht. Die Auswirkung von Funktionalisierungsmethoden wie auch unterschiedlicher Funktionalisierungsparameter auf die chromatographischen Eigenschaften wurde durch die Trennung von Standardsystemen (synthetische Peptide für Kationenaustauscher (CX), Oligonucleotide für Anionenaustauscher (AX)) untersucht. Die untersuchten Trennmedien zeigten generell gute Trenneigenschaften und ein klarer Einfluss der Funktionalisierungsparameter darauf wurde festgestellt. Abschließend wurde die klinische Anwendbarkeit von miniaturisierten CX-Monolithen untersucht. Es konnte eine Methode zur online-Festphasenextraktion von Imiquimod in Gewebsflüssigkeiten entwickelt werden, die gute Ergebnisse zeigt.

1. Aim of this work.....	6
2. Introduction.....	7
2.1. Chromatography.....	7
2.1.1. Types of chromatography.....	7
2.1.2. Chromatographic parameters.....	10
2.2. Chromatographic separation media	14
2.2.1. Packed media.....	15
2.2.2. Monolithic media.....	18
2.3. Ring-opening metathesis polymerisation for the preparation of monolithic separation media.....	20
2.3.1. Mechanism.....	20
2.3.2. Initiators.....	21
2.4. Surface modification of monoliths.....	24
2.4.1. Copolymerisation of functional monomer.....	24
2.4.2. Post-polymerisation functionalisation.....	24
2.4.3. Imprinting techniques.....	25
2.4.4. Production of non-functional and functional monoliths via ROMP.....	25
3. Experimental.....	27
3.1. General information.....	27
3.2. Materials & equipment.....	28
3.3. Methodology	29
3.3.1. Generalities	29
3.3.2. Chromatographic evaluation of CX monoliths	29
3.3.3. Chromatographic evaluation of AX monoliths	32
3.3.4. Chromatographic evaluation of RP-monoliths.....	34
3.3.5. Online-SPE of imiquimod.....	35
4. Results & Discussion.....	41
4.1. Chromatographic evaluation of CX monoliths.....	42
4.1.1. Optimisation of chromatographic conditions.....	43
4.1.2. Influence of the functionalisation parameters on the separation performance... 44	
4.1.3. Evaluation of hydrophobicity.....	51
4.2. Chromatographic evaluation of AX-monoliths.....	54
4.2.1. Optimisation of the separation conditions.....	55
Influence of the functionalisation parameter on the separation performance.....	57
4.2.3. Evaluation of the hydrophobicity.....	62
4.4. CX-monoliths for online-SPE of imiquimod	65
4.4.1. Method development for online-SPE of imiquimod with CX-monoliths	66
4.4.2. Evaluation of the method for online-SPE of imiquimod	70
4.4.3. Online-SPE of imiquimod in human biofluids	75
5. SUMMARY.....	77
6. References.....	79
List of Publications and Posters.....	83

Abbreviations

<i>A...</i>	<i>Symmetry parameter</i>
<i>ACN...</i>	<i>Acetonitrile</i>
<i>AX...</i>	<i>Anion exchange</i>
<i>B...</i>	<i>Symmetry parameter</i>
<i>ap...</i>	<i>Capillary</i>
<i>CEC...</i>	<i>Capillary electro-chromatography</i>
<i>CV...</i>	<i>Relative standard-deviation</i>
<i>CX...</i>	<i>Cation exchange</i>
<i>DMN-H₆...</i>	<i>1,4,4a,5,8,8a-hexahydro-1,4,5,8-exo-endo-di-methanonaphthaline</i>
<i>DVB...</i>	<i>Di-vinyl-benzene</i>
<i>ER...</i>	<i>Extraction recovery</i>
<i>F...</i>	<i>Flow velocity</i>
<i>FDA...</i>	<i>Food and Drug administration</i>
<i>H, HEPT...</i>	<i>Height equivalent of one theoretical plate</i>
<i>HSA...</i>	<i>Human serum albumin</i>
<i>id...</i>	<i>Inner diameter</i>
<i>IEX...</i>	<i>Ion exchange chromatography</i>
<i>ISF...</i>	<i>Interstitial fluid</i>
<i>K...</i>	<i>Permeability</i>
<i>k'...</i>	<i>Capacity ratio</i>
<i>L...</i>	<i>Column length</i>
<i>LC...</i>	<i>Liquid Chromatography</i>
<i>LOQ...</i>	<i>Limit of quantification</i>
<i>M...</i>	<i>Molarity</i>
<i>ME...</i>	<i>Matrix effect</i>
<i>MS...</i>	<i>Mass spectroscopy</i>
<i>N...</i>	<i>Plate number</i>
<i>NBE...</i>	<i>Norborn-2-ene</i>
<i>NBEA...</i>	<i>7-Oxanorborn-2-ene-5,6-dicarboxylic anhydride</i>
<i>NBEDM...</i>	<i>7-oxanorborn-2-ene-5-(N,N-dimethyletyl) carbonylamide</i>
<i>PMA...</i>	<i>Polymethacrylate</i>
<i>PS...</i>	<i>Polystyrene</i>

<i>r...</i>	<i>Radius</i>
<i>R...</i>	<i>Resolution</i>
<i>ROMP...</i>	<i>Ring-opening metathesis polymerisation</i>
<i>RP...</i>	<i>Reversed phase</i>
<i>RT...</i>	<i>Room temperature</i>
<i>S...</i>	<i>Symmetry</i>
<i>SEC...</i>	<i>Size exclusion chromatography</i>
<i>SPE...</i>	<i>Solid phase extraction</i>
<i>t ...</i>	<i>Retention time of peak x and x + 1</i>
<i>t₀...</i>	<i>Hold-up time</i>
<i>t_{R1}...</i>	<i>Total retention time</i>
<i>t'_{R1}...</i>	<i>Adjusted retention time</i>
<i>TFA...</i>	<i>Trifluoro- acetic acid</i>
<i>w_{1/2}...</i>	<i>Peak width of that peaks at 50% peak height</i>
<i>Δp...</i>	<i>column pressure drop</i>
<i>α...</i>	<i>Relative retention time</i>
<i>η ...</i>	<i>Viscosity</i>

1. Aim of this work

Modern analytical questions get more and more complicated because of the increasing demands of biotechnology, medicine and related sciences. To meet these higher and higher standards, the trend for chromatographic systems goes towards miniaturised separation media. The main advantage of miniaturised systems - capillary (cap) and nano high performance liquid chromatography (HPLC) - is the dramatic increase of sensitivity as well as the safe and simple possibility for online coupling with mass spectroscopy (MS), which makes the splitting of the eluate unnecessary. Also the saving of solvent and therefore saving of costs and environmental protection is an advantage of this evolution. Because of the fact that packing gets much more complicated with decreasing column diameter recent developments in chromatographic separation media went from packed columns to monolithic phases.

One attempt to produce monolithic media represents ring-opening metathesis polymerisation (ROMP) ^[1]. It has been described in many studies for the preparation of non-functional and functional monolithic separation media. Up to the present the influence of the terms of polymerisation as well as the functionalisation of ROMP-derived media on the material and chromatographic properties had been investigated analytical columns of inner diameters (id) ≥ 3 mm. ^[2, 3]. Further studies determined the impact of downscaling of the id of non-functional monolithic columns to morphology and therefore to separation performance ^[4, 5, 76].

So far, the chromatographic properties of miniaturised functionalised monolithic columns haven't been investigated. The evaluation of the influence of different functionalisation parameter of ROMP-derived monolithic columns on the chromatographic properties using selected standards was the main aim of this work. Also their applicability in clinical research should be investigated through the online-solid phase extraction (online-SPE) of imiquimod in human biofluids.

2. Introduction

Because this work bases on chromatography with monolithic columns, it will be necessary to give an introduction in the fundamentals of chromatography in the following chapters; special points of interest for this work as applied media and techniques will be focused.

2.1. Chromatography

In general, chromatography means physical and chemical methods to separate diverse compounds through dispersion between a stationary and a mobile phase. Because of differences in the mobility, the compounds of a sample are separated into discrete 'bands' that can be analysed qualitative and quantitative.

Chromatographic methods can be divided according to two aspects. The first one is basing on the manner of the contact between mobile and stationary phase (e.g. column chromatography, planar chromatography), the second, more basic one, differs the nature of the phases and the kinds of equilibriums, which are involved in the transfer of the dissolved substances. There are three main categories: liquid-, gas- and supercritical fluid chromatography.

2.1.1. Types of chromatography

Referring to the second aspect, six separation mechanisms will be described in detail.

2.1.1.1. Adsorption chromatography

In adsorption chromatography, the stationary phase is an adsorbent; separation happens through repeated steps of absorption/desorption. The mobile phase transports different compounds which become adsorbed by the stationary phase through differently strong physical forces (e.g. van der Waals - forces, ionic forces).

But these forces may not be too strong, because otherwise the equilibrium will not be achieved because desorption can't happen. Adsorption balances depend on the concentrations of the compounds in the mobile phase, also on the temperature and the ratio of the amount of adsorbent to amount of adsorbable compound.

2.1.1.2. Distribution chromatography

In distribution chromatography the separation is based on different solubilities of substances in both phases, stationary and mobile. In common, the distribution-law from Nernst is applied in the case of the distribution of a compound between two phases.

$$k = \frac{c_S}{c_M} \qquad \text{Equation 1}$$

c_S ... molar concentration of the analyte in the stationary phase

c_M ... molar concentration of the analyte in the mobile phase

The distribution coefficient k of a compound is the equilibrium-constant of a distribution-balance. It depends on the manner of the phases, temperature and pressure. Only compounds with clearly different k -values can be separated with distribution-chromatography.

2.1.1.3. Ion-exchange chromatography

In this method, the stationary phase has an ionic charged surface. Only complementary charged substances can be separated, the higher the difference in the charge is, the tighter the compound will be bound, and the longer is the retention-time. Aqueous solutions and buffered solvents with assessable pH-value and polarity (for the control of retention times) are used as mobile phases in ion-exchange chromatography (IEX). Mainly this method was used in this work.

2.1.1.4. Ion-pair chromatography

This kind of chromatography is an alternative to ion-exchange chromatography. Often mixtures of acids, bases and neutral substances can't be separated with IEX-chromatography techniques. In this case ion-pair chromatography is applied. Stationary phases for reversed phase (RP) chromatography are used, and an ionic organic compound is added to the mobile phase, which builds an ionic pair with the complementary charged substance. This pair is -chemically considered - a salt, but in chromatography it acts like a non-ionic organic molecule, which can be separated with RP-chromatography.

2.1.1.5. Size-exclusion chromatography

Size-exclusion chromatography (SEC), also called exclusion chromatography or gel-chromatography is a technique, in which the separation column is filled with a stationary phase with a defined pore-size. Separation in SEC works completely different to the previous methods. SEC doesn't use a physical force; it separates substances because of their different hydrodynamic volume, the stationary phase works like a 'sieve'. The separation mechanism bases on different penetration depths and dwell periods of the sample molecules in the pores of the separation material.

2.1.1.6. Affinity chromatography

This kind of chromatography bases on the feature of biological macromolecules to bind specific and reversible to other substances (ligands). Interactions that are useable for affinity-chromatography exist, for example, between antibody and antigen, enzyme and substrate (-analogue), enzyme and co-enzyme, and so on. Precondition is a covalent, irreversible bond of the ligand to a water-insoluble matrix-polymer. The chosen compound needs a high specificity to the immobilized ligand, while all other substances of the sample mixture pass the column without any interaction.

2.1.2. Chromatographic parameters

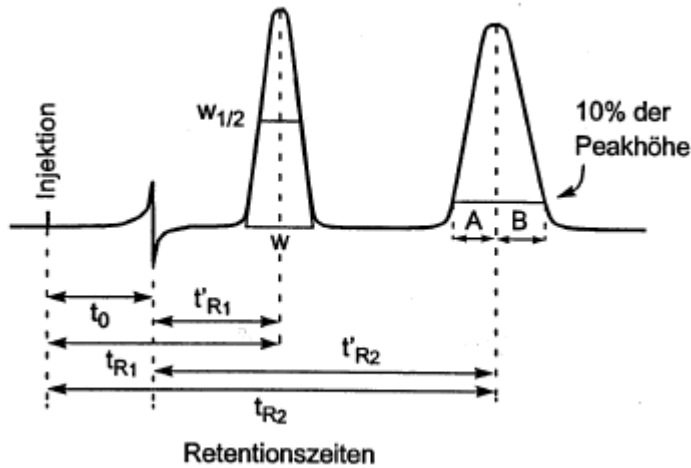


Figure 1: Chromatographic parameters of a chromatogram ^[6].

2.1.2.1. Hold-up time t_0

The hold-up time is that time, an inert substance (with no interaction to the stationary phase) needs, to get from the injector to the detector.

2.1.2.2. Total retention time t_{R1}

This is the time that a substance needs to get from the injector to the detector.

2.1.2.3. Adjusted retention time t'_{R1}

The adjusted retention time is the time a substance stays in the stationary phase; it is the difference between total retention time and hold-up time.

$$t'_{R1} = t_{R1} - t_0$$

Equation 2

t_0 ... Hold-up time

t_{R1} ... Total retention time

2.1.2.4. Capacity ratio k'

The capacity ratio is a unique property of a given solute which is calculated from its corrected retention time as a means of identification. It depends on the used stationary and mobile phase, temperature, packing and so on.

$$k'_1 = \frac{t_{R1} - t_0}{t_0} \quad \text{Equation 3}$$

t_0 ... Hold-up time
 t_{R1} ... Total retention time

2.1.2.5. Relative retention α

This value, also called separation factor, is the ratio of two capacity ratios. The relative retention describes the ability of a chromatographic system to differ between two compounds. Temperature, the properties of mobile and stationary phase influence the relative retention.

$$\alpha = \frac{k'_2}{k'_1} \quad \text{Equation 4}$$

k'_1 ... Capacity ratio compound 1
 k'_2 ... Capacity ratio compound 2

2.1.2.6. Permeability K

The permeability of the separation column describes the porosity of the column, the permeability for a mobile phase and characterises the hydraulic resistance. It depends on the mobile phase, the temperature, column length and on the pressure. A change in the columns permeability indicates a change of the packing materials. (e.g. swelling).

$$K = \frac{F \cdot \eta \cdot L}{\Delta p \cdot r^2 \pi}$$

Equation 5

F...	Flow velocity
η ...	Viscosity
L...	Column length
Δp ...	Column pressure drop
r...	Radius

2.1.2.7. Plate number N

The plate number characterises the quality of the separation column. The higher the count, the more complicate sample mixtures can be separated.

$$N = 5,54 \left(\frac{t_{R1}}{w_{1/2}} \right)^2$$

Equation 6

t_{R1} ...	Total retention time
$w_{1/2}$...	Peak width at half height

2.1.2.8. Height equivalent of a theoretical plate (HEPT) H

The HEPT-value means the length of a virtual column, in which the chromatographic equilibrium between mobile and stationary phase is achieved. This value also serves as an indicator for the quality of a separation column. It depends on the size of the particles, the flow velocity, on the mobile phase and especially on the quality of the packing.

$$H = \frac{L}{N}$$

Equation 7

L...	Column length
N...	Plate number

2.1.2.9. Peak symmetry S

Symmetry is defined through a ratio of A and B (see figure 1) in which A is the distance between the peak front and the peak maximum and B the distance from the peak maximum to the peak ending. In the ideal case the symmetry has a value of 1. Values less than 1 mean fronting, higher than 1 means tailing.

It is calculated referring to two codes in a different way: The AIA-code defines A and B at 10% maximum peak height and calculates it with equation 8; the US/EU-code determines A and B at 5% maximum peak height and uses equation 9.

$$S = \frac{B}{A} \quad \text{Equation 8}$$

$$S = \frac{B + A}{2A} \quad \text{Equation 9}$$

A, B... Symmetry parameter, see Fig. 1

2.1.2.10. Resolution

The resolution R describes the distance of two adjoining peaks. It indicates the separation ability and is calculated referring to EU-code as following:

$$R = 1,18 \cdot \frac{t_{x+1} - t_x}{w_{x+1} + w_x} \quad \text{Equation 10}$$

t... Retention time of peak x and x + 1

w... Peak width of that peaks at 50% peak height

2.2. Chromatographic separation media

Stationary phases in HPLC should meet following demands ^[7]:

- Fast and efficient separation to minimise losses through biodegradation
- High, from flow independent capacity
- Low backpressure
- Potential for fast and easy scale-up and scale-down
- Same material for analytical and preparative applications
- Easy handling
- Stability
- High “batch-to-batch” reproducibility

A basic distinction is drawn between columns consisting of packed particles which consist of many single particles and monolithic columns, which are made of one continuous block. Particles as well as continuous structures differ in its morphology ^[8], whereas these can show different porosities as shown in figure 2.

Spheric particles

1) non-porous



1) porous layer



1) persistent porous



Monolithic phases

1) non-porous skeleton



1) porous skeleton



Figure 2: Morphology of separation media ^[8].

2.2.1. Packed media

In HPLC almost exclusively spherical materials are used nowadays, whereas the common particle diameter is around 3 to 10 μm . Table 1 lists the most common packed column types.

Table 1: Common packed column types ^[9].

Column type				
Characteristics	Packed analytical	High-speed	Microbore	Micro
Particle size, d_p [μm]	10	2-5	3-5	3-10
Inner diameter, i_d [mm]	4-5	4-5	1-2	0.04-0.3
Column length, L [cm]	20-30	4-10	10-200	50-300
Plate number N	10.000	10.000	30.000	100.000
Flow rate, u [cm^3/min]	1-2	1-2	0.01-1	0.001-0.1
Sample volume [μl]	10	10	0.5-5	0.1-1
Detector cell volume [μl]	8	8	1-4	0.5
Run time, t [min]	10-30	1-5	1-10	50-300

Particles can be made of inorganic materials as well as polymeric materials. Their different properties are listed in table 2.

Inorganic materials

Silica is the most common used carrier material in HPLC. It shows high mechanic stability and an easy derivatisation, which enables a lot of applications (RP chromatography, IEX-chromatography, SEC and much else besides). However, the big disadvantage of silica-phases is the restricted pH-range ability from 2 to 8.

Alumina shows the same positive physical attributes as silica and offers a greater pH-rangeability but fewer possibilities for surface-derivatisation.

Polymeric materials

Although polymethacrylates (PMA) and polystyrenes (PS) are compressible, they are applicable in HPLC. Mechanical attributes are worse than that from silica and alumina, furthermore they are very hydrophobic. On the other hand they are compatible with aqueous systems and organic solvents over the whole pH-range.

The main part of commercial available separation media basing on styrene consists of polystyrene, cross-linked with di-vinyl-benzene (PS-DVB); they are more hydrophobic than PMA. Chemical modifications of PS-basing separation materials are quite hard to achieve, in essence only sulfonation with sulfuric acid and nitration with nitric acid leads to a high yield. Derivatisation of materials basing on PMA is possible through the carboxylic acid groups of it.

Table 2: Overview of the properties of separation material in HPLC.

Parameter	Silica	Alumina	PS-DVB	PMA
Organic solvents	+++	+++	++	++
pH – range	+	++	+++	++
Swelling/shrinking	+++	+++	+	+
Pressure stability	+++	+++	++	+
Surface modifiable	+++	+	++	+++
Efficiency	+++	++	+	+

* +) sufficient, ++) good, +++) very good

Packed separation media sometimes show properties, which can affect the realisation of fast separations negatively. They are characterised by slow mass transfer that is bound to diffusion of the “virtual” stationary fluid-film around the particles. This leads to a big decrease of efficiency at high flow rates, especial for large molecules as proteins and peptides [10, 11]. Hence, it is attempted to develop separation media for faster and more efficient separations. To minimise the effect of diffusion, there where several attempts; for example decrease of particle diameter, which also means an increase of particle surface and shortened diffusion distances. But an enormous increase of the back pressure is the consequence of this try. Another attempt was done by Regnier et al. 1990 with the implementation of perfusion-chromatography [12]. The in this method used particles are porous; they have integrated pores with more than 1µm. Because the flow of the mobile phase through this pores, the convection-term increases at the expense of the diffusion-term of the mass-transfer. This leads to better separation performance.

But another limitation of packed columns is the interparticular void volume that can only be minimised with smaller particles, but never totally eliminated. So, different attempts for better mass transfer through elimination of void volumes have been worked out. One try was the use of separation media that possess a higher grade of continuity. Porous discs ^[13], stacked membranes ^[14], rolled-up cellulose ^[15] or woven matrices ^[16] have been implemented, but all showed an increase of the peak widths.

Because of these limitations, the trend in HPLC goes towards miniaturisation and micro-applications. The decrease of the column-dimensions offers a series of advantages as:

- Saving of solvents, therewith less pollution and costs
- Analysis of small sample volumes
- Safe and easy handling for coupling of LC/MS
- A drastic increase in sensitivity

But miniaturisation of packed columns has only limited applications in routine-analysis. Reasons for this are problems like increasing back pressure in LC (micro, cap, nano), building of gas-bubbles in CEC, difficulties with the reproducibility in the production of the columns and fragility of the capillaries. The two last-mentioned often are caused by frits, respectively frit-production.

Because of this limitations of packed media a different type of stationary phases, monolithic media, have been developed.

2.2.2. Monolithic media

Definition

Monolithic columns consist of one piece of a continuous, porous material that is hermetically sealed against the wall of a tube. So the stream of mobile phase cannot bypass any significant length of the bed but must percolate through it ^[39]. So the existence of interparticular void volumes is impossible.

Generally the major advantage of monolithic supports, whether in chromatography or in heterogeneous catalysis, is the fast mass transport that is achieved between the monolithic support (stationary phase, catalyst bed) and the surrounding liquid (mobile phase, reaction mixture). These transport phenomena are nowadays quite well understood ^[32]. Because of the special morphology, monolithic materials feature following characteristics:

- no particle synthesis
- no packing procedures
- no void volumes
- little back pressure and so higher flow rates
- increased mass transfer of the analyte from the mobile to the stationary phase

Today various products are available commercially, a list can be found in table 3.

Table 3: Commercial available monolithic products in chromatography ^[17].

Producer	Product	Shape	Chemistry	Separation modes
BIA	CIM disc	Disc, tube	PMA	Ion exchange, hydrophobic interaction Reversed phase, bioaffinity
Conchrom	CB silica plate	Disc	Modified silica	Ion exchange, reversed phase, normal phase
Sepragen	Seprisorb	Disc	Modified cellulose	Ion exchange
BioRad	UNO	Cylinder	PMA-based copolymers	Ion exchange
Merck	Chromolit h	Cylinder	Modified silica	Reversed phase
Dionex LC-Packings	Proswift	Cylinder	PMA, PS-DVB	Ion exchange, reversed phase
	Pepswift	Cylinder	PS-DVB	Reversed phase

History of monolithic media

The history of monoliths can be found in a number of reviews ^[18-22]. Monolithic materials go back to the late 1960s. Kubín et al. were the first to investigate alternatives to packed columns based of beaded polymers or inorganic oxides ^[23]. They developed methacrylate-based hydrogel-type materials with low degrees of cross-linking. Not unexpected, these materials were compressible and only allowed for comparatively low flow rates. A milestone in the development of these materials was the use of open-pore poly(urethane)-based materials which allowed for the separation of small analytes by means of HPLC ^[24, 25]. Their use as GC column was, however, restricted due their insufficient thermal stability (<200°C). Hjertén et al. published work on continuous beds consisting of acrylic acid and N,N-methylene bis(acrylamide) in the presence of a salt ^[26-28]. This material then was compressed within the confines of a chromatographic column and allowed for high flow rates. Parallel work by Belenkii et al. ^[29, 30] and Tennikova et al. ^[31] finally resulted in the birth of “monolithic” media. The development of monolithic materials still goes on, because of the limitations of packed media in LC, high performance LC (HPLC), capillary LC (cap-LC) and CEC.

Generally, there are two fields in which application of monolithic separation materials seems profitable. On the one hand, this is the realisation of extremely fast separations with very high flow rates, and on the other hand in miniaturisation of separation media, which would be exceedingly difficult with packed materials.

There are several attempts to synthesise monolithic separation media and many materials that are applied. Monoliths can be prepared of silica ^[33, 34, 35] or base on different polymers ^[21]. Also monolithic columns prepared of metal oxides ^[36] and carbon ^[37, 38] have been described; an excellent review is given elsewhere ^[39].

Polymer-based monoliths can be derived via different manners of polymerisation. This are thermally triggered free radical polymerisation, UV- or γ -irradiation induced polymerisation ^[40, 41], electron-beam polymerisation ^[42], polycondensation ^[43], polyaddition ^[44, 45] and the “living” polymerisation techniques TEMPO ^[66] and ROMP ^[1]; a review to give an insight into this wide field is listed ^[21].

2.3. Ring-opening metathesis polymerisation for the preparation of monolithic separation media

Under the mentioned polymerisation-techniques for the preparation of monoliths, ROMP ^[1] will be described in more detail, because of the easy possibility to use functional monomers which is of special interest for this work.

This reaction was first observed as a side reaction of the transition metal catalysed polymerisation of cyclo-olefines:

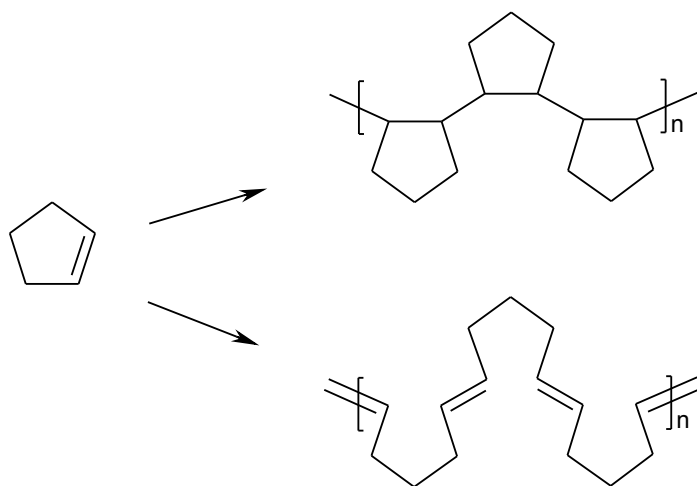


Figure 3: Formation of unsaturated linear polymers from cycloolefines as side-reaction ^[46].

2.3.1. Mechanism

The mechanism of this reaction has been a riddle for a long time and also the attempt to describe the reaction with a “paired mechanism” ^[50, 51] wasn’t able to win recognition. But 1970 Chauvin postulated a mechanism in which a metal-cyclobutano ring is formed and afterwards under formation of an olefin opened ^[52]. This mechanism achieved broad acceptance and was eventually accredited through the synthesis defined catalysts, which provided stable and well characterisable products ^[53].

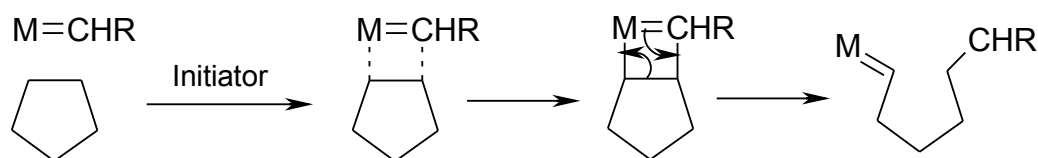


Figure 4: Chauvin reaction-mechanism of ROMP.

2.3.2. Initiators

ROMP-Initiators are essentially different to metathesis-catalysts (which are not able to polymerise cyclic olefins under ring opening), cause of the polarisation of metalcarbenes. Fischer-carbenes have a partial positive charged carben-carbon; ROMP-initiators (also called Schrock-initiators) show a partial negative charged carbon (see figure 5). Ligands substituted with nitrogen can increase the partial charge of the electrophilic metal-centre which leads to a higher reactivity.



Figure 5: Difference between Fischer- and Schrock-carbenes.

Schrock and later Grubbs synthesised stable metal-olefins that allowed the synthesis of well-defined substances; this leveraged ROMP. Cause of the position of the transition metal in the periodic table Grubbs- and Schrock initiators are significant different in their reaction- and polymerisation-behaviour. Schrock-initiators are made of transition metals of the VI to VII subgroup and show a very high ROMP-activity (which can be manipulated through the choice of the substituents). Disadvantage of Schrock-initiators is the high sensitivity to oxygen and protic functional groups. Grubbs-initiators basing on Ruthenium solve this problem, but have a drastic reduced reactivity and less living character of the polymerisation.

Polymers from metathesis polymerisation of cyclo-olefines keep the C-C double bound, and because of this they can form cis- and trans-stereo isomers. It is a matter of insertion mechanism in which the cyclic monomer is inserted in the growing polymer chain. This process is a reversible, entropy-controlled balance-reaction, which lies at the side of the polymer chain.

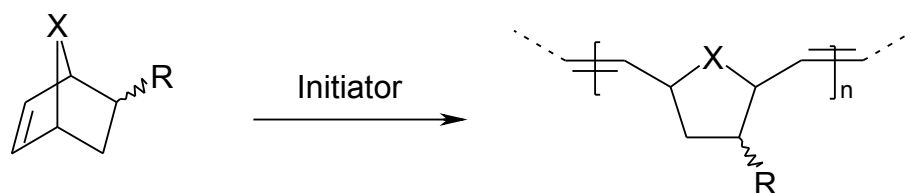


Figure 6: General reaction scheme of ring-opening metathesis polymerisation.

ROMP has a lot higher stereo-selectivity than metathesis polymerisation of acyclic olefins, so it is possible to manage the cis- or trans content of the polymerisation of cyclo-pentene with wolfram- and molybdenum-initiators and raise it up to 100%.^[47] Initiators of the Grubbs-type prefer the formation of trans-double bounds, Schrock-initiators can affect the configuration of the double bounds through the choice of the alcoxy-sustituents^[48, 49]. And because the structure of a polymer has a big influence on its physical properties (like melting point, elastic modulus, etc.) not only a high consistent cis- or trans configuration is important, but also the tacticity of the polymer units, which can also be controlled with the choice of the initiator.

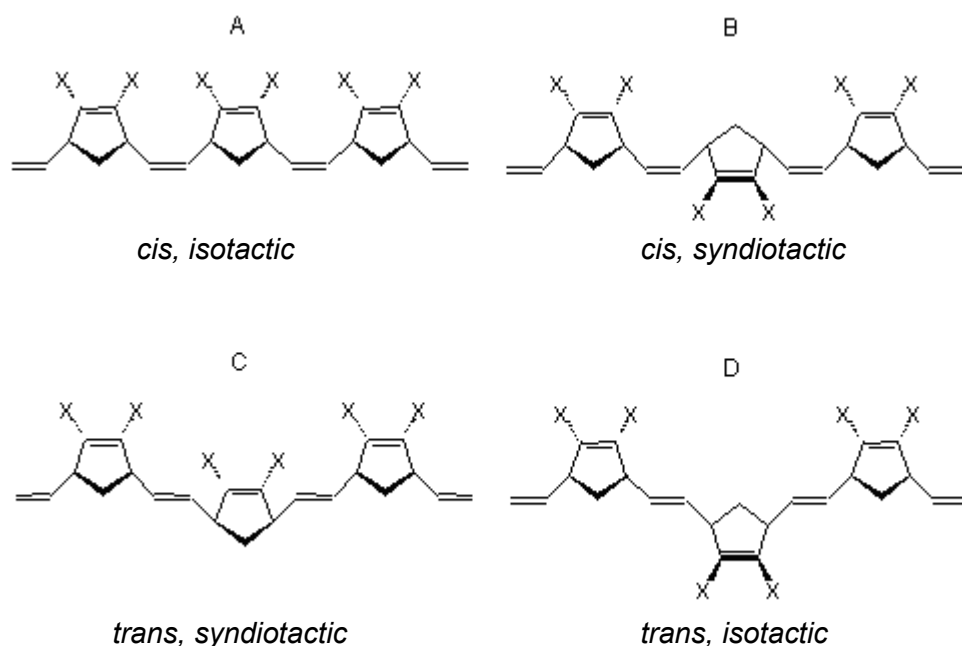


Figure 7: Possible regular structures of 2,3 – di-substituted norbornadiens.

ROMP shows some characteristic properties, leading to a special position among the classical types of polymerisation. With proper choice of the reaction parameters a 'living' polymerisation character can be achieved which opens new routes for synthesis. In this content 'living polymerisation' means a chain reaction with following properties:

- Molecular weight of the polymer is determined through the proportion of initiator to monomer
- Chain-initiation speed is much higher than chain-growing speed
- No chain-breakdown- or chain transfer-reactions
- Addition of new monomer leads again to chain growing

In the last years also radical and cationic polymerisations have been published; in the case of living radical polymerisation it's about stabilised radicals ^[54].

Because of the “living” character of these polymerisations it is possible to produce defined polymers and co-polymers, which show high homogeneities. This allows also the production of well-defined functional homo- or copolymers through the usage of functional monomer ^[55] and therefore gives easy access to functionalised monolithic columns.

2.4. Surface modification of monoliths

In general, there are three principle ways to produce polymer based monoliths with functional groups ^[18, 22, 56]. The first one is the co-polymerisation of functional monomers, the second post-polymerisation functionalisation, also called secondary functionalisation or grafting ^[57]. The third method is imprinting ^[58].

2.4.1. Copolymerisation of functional monomer

The easiest way to functional monoliths is to co-polymerise a functional monomer, the presence of this monomer during polymerisation will lead to a monolithic structure, that partly consists of the used functional monomer. There are two main disadvantages with this approach: The whole monolith synthesis must be elaborated for each different functional monomer, because of changes in the polarity of the monolithic backbone and as a result of this, also changes in the porosity. Secondly, the main part of the functional monomer is located within the non-porous micro globules, which means that this method is uneconomic in the case of expensive or hardly synthesisable monomers ^[59]. It also may lead to unfavourable swelling characteristics of the produced monolith, especially when used in gradient separations.

2.4.2. Post-polymerisation functionalisation

One approach is the transformation of the co-polymerised monomer into functional structures through chemical reactions ^[60-63]; also methods to graft functional monomer onto the monolithic surface have been developed ^[64, 65].

The major advantage of grafting techniques is the fact, that the parent monolithic system can be prepared from one optimised monomer / crosslinker / porogen system. Second, the polarity of the monolithic support isn't changed through the grafting procedure that much as for chemical transformations – which is important for applications in separation science. The special nature of the living polymerisation in some polymerisation techniques (TEMPO ^[66], ROMP ^[1]) gives an easy access for grafted polymers, the simple add-on of functional monomer leads to functionalised polymers.

2.4.3. Imprinting techniques

Imprinting means the polymerisation around a special “mould”, so the produced polymer forms a type of ‘negative’ of the analyte-shape.

2.4.4. Production of non-functional and functional monoliths via ROMP

For the preparation of the monolithic structures; in terms of monomers and crosslinkers, norborn-2-ene (NBE), 1,4,4a,5,8,8a-hexahydro-1,4,5,8-*exo-endo*-dimethanonaphthalene (DMN-H₆), tris(norborn-5-ene-2-ylmethylenoxy)methylsilane as well as cyclooctene and tris(cyclooct-4-ene-1-yloxy)methylsilane have been used ^[67-72]. After deactivation of the polymerisation catalyst the obtained monoliths can be used in RP-chromatography, see figure 8.

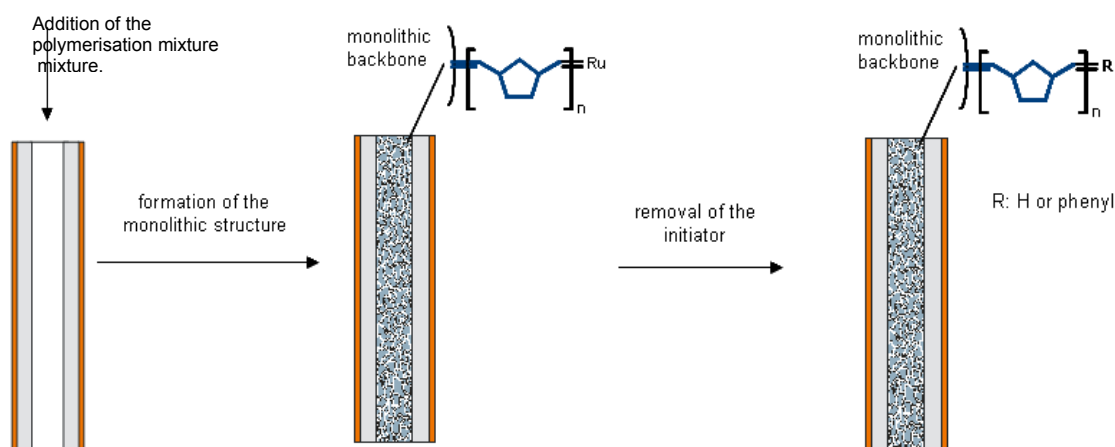


Figure 8: Reaction schema for preparation of a ROMP-derived RP-monolith.

Utilizing the “living” character of ROMP, there is an easy way to obtain functional columns; two functionalisation techniques have been successfully applied. These techniques are *in-situ* grafting and *post-synthesis* grafting.

2.4.4.2. *In-situ* grafting

The controlled “living” [73, 74] polymerisation mechanism offers a perfect access to functionalisation, that can be performed *in-situ*. In fact, the active initiator-sites can successfully be used for derivatisation after the formation of the monolithic backbone is complete. Using the initiator covalently bound to the monolith surface, several functional monomers can be grafted onto it by simply passing solutions thereof through the monolith [3, 75]; tentacle-like polymer chains attached to the surface are formed, see figure 9 [76].

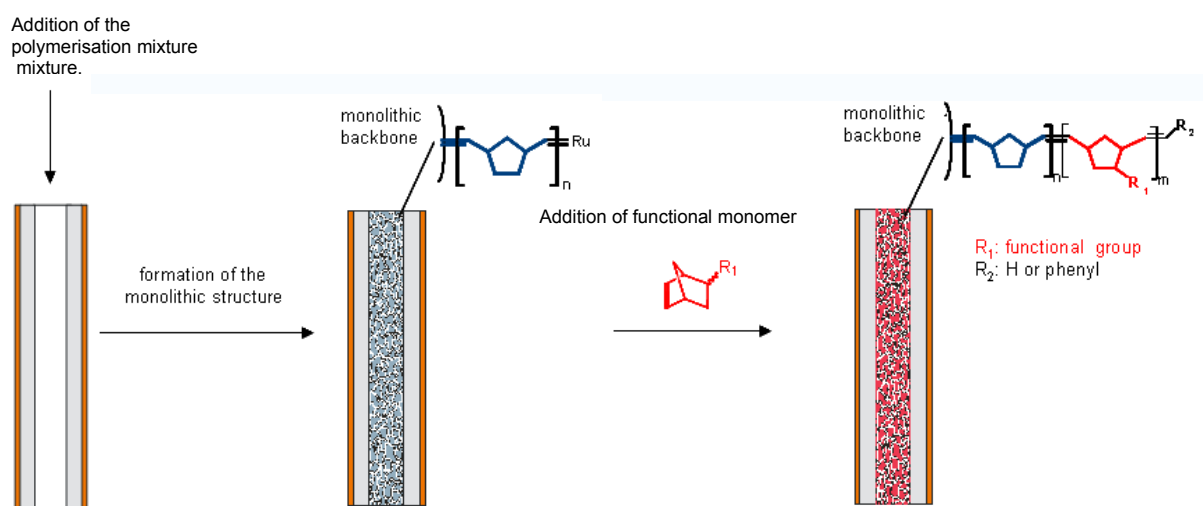


Figure 9: Reaction schema for preparation of an *in-situ* grafted ROMP-derived monolith.

2.4.4.3. *Post-synthesis* grafting

To increase the grafting yields, a *post-synthesis* grafting method can be applied [77]. In this case, after the formation of the monolith, an additional catalyst is added, which reacts with the double bounds of the monolithic backbone and activates them. So more active grafting-sites are formed which can react with the functional monomer passing by while functionalisation.

3. Experimental

3.1. General information

ROMP-derived capillary monoliths of 200 μm id comprising cationic and anionic functional groups have been provided. The preparation of those included the polymerisation of NBE as monomer and DMN-H₆ as cross-linker; a Grubbs catalyst 1st generation ($\text{Cl}_2(\text{P Cy}_3)_2\text{Ru}=(\text{CHPh})$) acted as ROMP-active initiator, isopropanol served as macroporogen and toluene as microporogen [76]. The functionalisation was performed through grafting of 7-oxanorborn-2-ene-5,6-dicarboxylic anhydride (for cation exchange monoliths (CX)) and 7-oxanorborn-2-ene-5-(N,N-dimethylethyl) carbonylamide (for anion exchange monoliths (AX)) for two different techniques. The grafting methods were *in-situ* grafting and *post-synthesis* grafting. Also different functionalisation conditions have been applied; these functionalisation parameters (techniques and conditions) resulted in monoliths with different ion exchange capacities (see table 4 and 5).

Table 4: Overview provided monoliths CX.

Monolith	Grafting technique	NBE in grafting solution [%]	Post-synth. grafting Temp. [°C]	Post-synth. grafting catalyst	Funct. Temp. [°C]	Capacity [$\mu\text{equiv/ml}$]
M1	<i>In-situ</i>	-	-	-	RT	0.22
M2	<i>In-situ</i>	-	-	-	40	0.83 \pm 0.19
M3	<i>Post-synthesis</i>	-	RT*	Grubbs 1 st	40	1.89

*RT... Room temperature

Table 5: Overview provided monoliths AX.

Monolith	Grafting technique	NBE in grafting solution [%]	Post-synth. grafting Temp. [°C]	Post-synth. grafting catalyst	Funct. Temp. [°C]	Capacity [$\mu\text{equiv/ml}$]
M4	<i>In-situ</i>	0	-	-	40	0.09 \pm 0.01
M5	<i>In-situ</i>	15	-	-	40	0.36
M6	<i>Post-synthesis</i>	-	RT	Grubbs 1 st	40	0.17 \pm 0.01
M7	<i>Post-synthesis</i>	-	60	Grubbs 1 st	40	0.31 \pm 0.01
M8	<i>Post-synthesis</i>	-	RT	Hoveyda 2 nd	40	0.65
M9	<i>Post-synthesis</i>	-	60	Hoveyda 2 nd	40	1.22 \pm 0.13

3.2. Materials & equipment

Table 6: Materials.

Description	Provider
fused silica capillaries, 200 µm i.d.	J&W
Coupling adapter	Upchurch
Peek sleeves	Upchurch
Ferules	Upchurch
Microliter syringe (50µl)	Hamilton gastight

Table 7: Equipment.

Description	Provider
Autosampler FAMOS	LC Packings
HPLC-pump Ultimate	LC Packings
Calibrator cartridges for cap-HPLC CAP-300; CAP-500; MIC-1000	LC Packings
Ultimate UV-detector	LC Packings
Flow cell (45 nl)	LC Packings
Software	Chromeleon ver. 6.70
PH-meter	Thermo Orion

Table 8: Chemicals for the preparation of the mobile phase.

Description	Provider
Water HPLC grade	from Elix Millipore system, Fluka
Acetonitrile Chromasolv	Sigma Aldrich
Trifluoro acetic acid (TFA)	Fluka
Di-sodium hydrogen phosphate-2- hydrate (Na ₂ HPO ₄ ·2H ₂ O)	Riedel-de Haën
Sodium dihydrogen phosphate-2- hydrate (NaH ₂ PO ₄ ·2H ₂ O)	Riedel-de Haën
Ammonium acetate (NH ₄ CH ₃ COO)	Fluka
Sodium chloride (NaCl)	Fluka
Acetic acid (CH ₃ COOH)	Riedel-de Haën
Ammonium hydroxide (NH ₄ OH)	Fluka
Helium	Air Liquid

Table 9: Chemicals for standards.

Description	Provider
Synthetic peptides	piCHEM
Oligothymidines, ammonium salt (d(pT) ₁₂₋₁₈)	Sigma Aldrich
Imiquimod	Sigma Aldrich
Physiological NaCl-solution; 0.9M	Fresenius

3.3. Methodology

3.3.1. Generalities

All chromatographic separations were carried out at a column flow of 10 μ l/min. Because of the different back pressure of the monoliths the column flow had to be adjusted via changes of the pump flow and the use of different calibrator cartridges for cap-HPLC. Therefore the pump flow was different for each monolith. The column flow was checked and, if necessary, adjusted at least 2 times a day using a stopwatch and a 50 μ l syringe.

The column temperature was room temperature for all measurements (air-conditioned room) and the injection volume was 2 μ l unless otherwise noted.

Before each measurement the used column was conditioned for 30 minutes (except from the online-SPE of imiquimod) and all used mobile phases have been degassed with helium while HPLC-application.

3.3.2. Chromatographic evaluation of CX monoliths

The CX-monoliths were investigated in their separation performance of a peptide-mixture. The detection happened via UV-detector at wavelengths of 190, 210, 220 and 280 nm; but only the data of wavelength 220 nm were used for evaluation. The used calibrator cartridges were CAP-300 and CAP-500.

3.3.2.1. Standards

To characterise the monoliths with CX properties following synthetic peptide standard has been prepared. The amino acid sequence of each peptide is listed in table 10.

Table 10: Used synthetic peptides.

Name	Amino acid sequence
Peptide 1 (P1)	Ac-Gly-Gly-Gly-Leu-Gly-Gly-Ala-Gly-Gly-Leu-Lys-NH ₂
Peptide 2 (P2)	Ac-Lys-Tyr-Gly-Leu-Gly-Gly-Ala-Gly-Gly-Leu-Lys-NH ₂
Peptide 3 (P3)	Ac-Gly-Gly-Ala-Leu-Lys-Ala-Leu-Lys-Gly-Leu-Lys-NH ₂
Peptide 4 (P4)	Ac-Lys-Tyr-Ala-Leu-Lys-Ala-Leu-Lys-Gly-Leu-Lys-NH ₂

Ac... Acetyl group

10 mg of the respective synthetic peptide were dissolved in 1 ml water, the resulting solution (concentration 10µg/µl) was the main stock and stored at -20°C. For P1 and P2 aliquots were prepared through dilution of 25µl stock solution with water in a 5 ml volumetric flask; therefore the aliquot-concentration was 50ng/µl. P3 and P4 aliquots were prepared through diluting 50 µl of the stock solution with 950 µl water; the end concentration was 500ng/µl. These peptide standards were divided into aliquots of 50µl and stored at -80°C.

For the chromatographic evaluation a mixture of these peptides has been prepared through mixing of the necessary amounts of the aliquots. Amounts of the peptide aliquots as well as the final concentrations for the synthetic peptides are listed in table 11.

Table 11: Composition of the mixed standard.

	P1	P2	P3	P4	Buffer	H ₂ O
Aliquote volume [µl]	200	100	25	20	5	150
Concentration [ng/µl]	20	10	25	20	1mM	-

Buffer... 100mM pH 7, preparation see below

3.3.2.2. Eluents

The mobile phase for the evaluation of the separation performance of CX-monoliths consisted of a mixture of ACN, water and NaCl, buffered to a pH of 7.

The used HPLC-device featured four solvent channels (A, B, C, D), they were used as follows:

Channel **A**: Water.

Channel **B**: ACN.

Channel **C** consisted of phosphate buffer 10mM, pH 7. It was prepared through dissolving of 0.178g $\text{Na}_2\text{HPO}_4 \cdot 2\text{H}_2\text{O}$ in 100ml water and bit by bit addition to a prepared solution of 0.156g $\text{NaH}_2\text{PO}_4 \cdot 2\text{H}_2\text{O}$ in 100 ml water till a pH-value of 7.0 was reached.

Channel **D** was NaCl in a concentration of 2M, prepared through a weighted sample of sodium chloride of 23.38 g dissolved in 200ml of water. In table 12 the contents of the solvent channels are listed.

Table 12: Contents of the mobile phases for CX-monoliths.

Channel	A	B	C	D
H ₂ O	100%	-	100%	100%
ACN	-	100%	-	-
Buffer pH 7	-	-	10mM	-
NaCl	-	-	-	2 M

3.3.2.3. Elution gradients

This gradient was performed for isocratic ACN-contents of 0, 10, 20, 30 and 40%; eluent C was kept at 10% over the whole time. The separation of the mixed standard was achieved through a gradient of solvent D, NaCl 2M; the content of channel D was continuously increased in 7.5 minutes up to a percentage of 38%. This amount of D was kept isocratic for 10 minutes, and then decreased to 0 within 1 minute and hold for 41.5 minutes to condition the columns. It has to be noted, that the maximum content of channel D was 25% when measuring at 40% ACN because of the bordered solubility of NaCl for this content of ACN. The slope of the NaCl-gradient was kept constantly through shortening of its duration to 5 minutes in this case. The applied solvent-gradient is listed in table 13.

Table 13: Solvent gradient for CX separations; 30% ACN isocratic.

Time [min]	A [%]	B [%]	C [%]	D [%]
0 – 7.5	60-22	30	10	0-38
7.5 – 17.5	22	30	10	38
17.5 – 18.5	22-60	30	10	38-0
18.5 – 60	60	30	10	0

3.3.3. Chromatographic evaluation of AX monoliths

The AX-monoliths were investigated in their separation performance of a prepared standard-mixture consisting diverse oligonucleotides. The detection again occurred via UV-detection, the recorded wavelengths were 190, 210, 254 and 260nm whereas only the signal of 254nm was used for evaluation. The used calibrator cartridges were CAP-500 and MIC-1000.

3.3.3.1. Standards

To characterise the provided AX monoliths following standard have been prepared. 20µg d(pT)₁₂₋₁₈ were dissolved in 500µl of water (= stock solution, stored at -20°C). Out of this, 200µl were drawn and filled up to 5ml with H₂O. This solution was divided into aliquots of 50µl each and stored at -80°C, the end concentration of the aliquots was therefore 16ng/µl. The used standard-concentration of 8ng/µl was obtained through a 1:1 dilution of an aliquot with water.

3.3.3.2. Eluents

The mobile phase for the evaluation of the separation performance of AX-monoliths consisted again of a mixture of ACN, water and NaCl, buffered to a pH of 7.

The four channels of the HPLC-system were used as follows:

Channel **A**: water.

Channel **B**: ACN.

Channel **C** contained phosphate-buffer 100mM pH7. For this, 1.78g Na₂HPO₄·2H₂O were dissolved in 100 ml water and added bit by bit to an already prepared solution of 1.56g NaH₂PO₄·2H₂O in 100 ml water till a pH-value of 7.0 was reached.

Channel **D** featured a solution of 1M NaCl. It was prepared through dissolving of 11.69 g NaCl in 200ml of water. In table 14 the contents of the solvent channels for AX-measurements is listed.

Table 14: Contents of the mobile phases for AX-separations.

Channel	A	B	C	D
H ₂ O	100%	-	100%	100%
ACN	-	100%	-	-
Buffer pH 7	-	-	100 mM	-
NaCl	-	-	-	1 M

3.3.3.3. Elution gradients

The gradient was performed for various isocratic contents of ACN (0, 5, 10, 15, 20, 25, 30%), channel C was kept at 5% isocratic. The separation of the d(pT)₁₂₋₁₈ standard was achieved through a gradient of solvent D (NaCl 1M). The content of channel D was increased in 1 minute to 5%, and then continuously rose to 30% in 12.5 minutes. After the slope of D its content was kept isocratic for 3.5 minutes, and then decreased to 0 within 1 minute. From then, the mobile phase consisted to 100% of water.

It has to be noted, that the maximum content of channel D was increased to 50% for the monoliths M8 and M9, otherwise the standard wasn't possible to elute. The slope of the NaCl-gradient was kept constantly of course through prolongation of its duration to 21 minutes. The applied solvent-gradient is listed in table 15.

Table 15: Solvent gradient for AX-separations at 30% ACN isocratic.

Time [min]	A [%]	B [%]	C [%]	D [%]
0-1	65-60	30	5	0-5
1 – 13.5 *	60-35	30	5	5-30 *
13.5 – 17	35	30	5	30 *
17 – 18	35-100	30-0	5-0	30-0 *
18 – 70	100	0	0	0

*... Changed for M8 and M9 as above mentioned

3.3.4. Chromatographic evaluation of RP-monoliths

The chromatographic behaviour of the peptide standard and the oligonucleotide standard on a RP-monolith at two different pH-values (pH 7 and pH 2) has been investigated. Again, an UV-detector recorded the wavelengths 190, 210, 254 and 280nm whereas only the signal of 254nm was used for evaluation. The used calibrator cartridges were CAP-500 and MIC-1000.

3.3.4.1. Eluents

The mobile phase consisted of water, buffer with the respective pH and an ACN-gradient.

pH 7: Channel **A**: water.

Channel **B**: ACN.

Channel **C** contained buffer solution 100mM pH 7. It was prepared through dissolving of 1.78g $\text{Na}_2\text{HPO}_4 \cdot 2\text{H}_2\text{O}$ in 100ml water and bit by bit addition to an already prepared solution of 1.56g $\text{NaH}_2\text{PO}_4 \cdot 2\text{H}_2\text{O}$ in 100 ml water till a pH-value of 7.0 was reached. Channel **D** was not used.

pH2: Channel **A** provided a solution of 0.05% TFA in water.

Channel **B** contained ACN with 0.05% TFA. They were prepared through addition of 50 μl TFA to water respective ACN and filling up this solution in a volumetric flask up to 100ml.

Channel **C** and **D** weren't used.

3.3.4.2. Elution-gradients

The applied gradient for RP-measurements comprised an isocratic content of the respective pH-solution and an ACN elution gradient, beginning at 0% ACN, then rose up to 50% in 15 minutes. Further it was risen up to 80% in 1 minute and kept constantly at this content for 13 minutes. In minute it was finally decreased again to 0% and hold for 20 minutes to condition the column. Table 16 shows the solvent gradient for RP-investigations.

Table 16: Solvent gradient for RP-measurement.

Time [min]	A [%]	B [%]	C [%] *
0-15	99-49	0-50	1
15 – 16	49-19	50-80	1
16 – 29	19	80	1
29 – 30	19-99	80-0	1
30 – 50	99	0	1

*... for pH2 measurements channel C wasn't used

3.3.5. Online-SPE of imiquimod

The chromatographic behaviour of standard-solutions of the drug imiquimod as well as of human serum albumin (HSA) on a RP- and a CX-column have been investigated.

Detection of imiquimod as well as HSA happened via UV-detector at wavelengths of 190, 210, 220 and 280 nm; but only the data of wavelength 220 nm was used for evaluation. The used calibrator cartridge was CAP-500.

3.3.5.1 Standards

Imiquimod: 8.0mg were dissolved in 40ml of a solution containing 80% ACN and 20% H₂O, this led to a concentration of 200ng/μl. 4 ml of the resulting stock solution have been divided into aliquots of 100μl each, the remaining was disposed. The relatively high volume of 40 ml solution was necessary because of the poor solubility of Imiquimod in the used solvents.

The imiquimod-standard for the investigations of the chromatographic behaviour was prepared through dilution of the aliquots with water to 10ng/μl. The used standards for online-SPE with concentrations of 10, 50, 100, 150 and 200ng/μl (S1 to S5) were prepared through dilution of the aliquots with water as listed in table 17.

HSA: To prepare the HSA-stock solution for the investigations of the chromatographic behaviour, 50mg HSA were dissolved in 5ml water to receive the

HSA-stock with a concentration of 1% HSA, respectively 10µg/µl. This was stock was diluted with water to the standard concentration of 100ng/µl.

Simulated matrix: The matrix for the online-SPE-development was prepared through dissolving 50mg HSA in 5 ml physiological NaCl-solution; the 2-fold concentrated simulated matrix through dissolving of 100mg HSA and 0.292g NaCl in 5ml of water.

3.3.5.2. Sample preparation

3.3.5.2.1. Protein precipitation

40 µl of the simulated matrix were put first in a 200µl PCR-tube and spiked with different amounts of ACN. The precipitation of HSA was observed and the investigations noted. In table 17 the different precipitation conditions are listed.

Table 17: HSA-precipitation tests of simulated matrix.

Solvent	80% ACN	70% ACN	60% ACN	50%ACN	40% ACN
1% HSA-stock[µl]	40	40	40	40	40
Water [µl]	0	20	40	60	80
ACN [µl]	160	140	120	100	80

3.3.5.2.2. Recovery / accuracy evaluation

To evaluate the recovery of the sample preparation as well as to determine the accuracy of the online-SPE measurements three sample-series have been prepared, A-, B-, and C-samples. Their preparation happened as follows, each sample was prepared 3 times.

Preparation of A-samples (Matrix spiked, see table 18):

- 10µl matrix (2-fold concentrated simulated matrix) in PCR-tube
- Spike with 10µl of the respective standard
- Addition of 80µl ACN,
- Vortex well
- Centrifugation for 15min at 13200 rpm
- Careful transfer of 90µl in a HPLC-vial with a 100µl glass insert
- Vortex well
- Sample analysis

Table 18: A-samples composition – simulated matrix spiked.

Sample No.	A1	A2	A3	A4	A5
sim. Matrix [μ l] (2x)	10	10	10	10	10
Standard*-Volume [μ l]	10	10	10	10	10
ACN [μ l]	80	80	80	80	80
Imiq. concentration [ng/ μ l]	1 ng / μ l	5 ng / μ l	10 ng / μ l	15 ng / μ l	20 ng / μ l

*... Standards 1-5

The sample preparation for real biofluid samples happened the same way, except of the used matrix, which was 10 μ l of the respective human biofluid (interstitial fluid (ISF) respective blood serum) instead of 2-fold concentrated simulated matrix.

Preparation of B-samples (simulated matrix; not spiked, see table 19):

- 20 μ l matrix (water) in PCR-tube
- Addition of 80 μ l ACN,
- Vortex
- Centrifugation for 15min at 13200 rpm
- Careful transfer of 90 μ l in a HPLC-vial with a 100 μ l glass insert
- Spike with 10 μ l of the respective standards (see table 17)
- Vortex well
- HPLC-analysis

Table 19: B-samples composition – simulated matrix not spiked.

Sample No.	B1	B2	B3	B4	B5
Simulated Matrix [μ l]	20	20	20	20	20
ACN [μ l]	80	80	80	80	80
Standard*-Volume [μ l]	10	10	10	10	10
Imiq. concentration [ng/ μ l]	1 ng / μ l	5 ng / μ l	10 ng / μ l	15 ng / μ l	20 ng / μ l

*... Standards 1-5

The preparation of C-samples (matrix water; not spiked, see table 20) happened the same way, except of the fact, that the 20 μ l used matrix consisted of water.

Table 20: C-samples composition - water not spiked.

Sample No.	C1	C2	C3	C4	C5
water [µl]	20	20	20	20	20
ACN [µl]	80	80	80	80	80
Standard*-Volume [µl]	10	10	10	10	10
Imiq. concentration [ng/µl]	1 ng / µl	5 ng / µl	10 ng / µl	15 ng / µl	20 ng / µl

*... Standards 1-5

3.3.5.3. Eluents

For the evaluation of the chromatographic behaviour of imiquimod and HSA, the mobile phase consisted of water and ACN in various percentages (0-80%) and pH-values (pH 2, 3, 5, 7, 8). The solvent channels were used as follows:

Channel **A** water.

Channel **B** ACN.

Channel **C** provided a solution of 0.25% TFA in water, with a pH about pH 2. It was prepared through addition of 250µl TFA to water, and filling up this solution in a volumetric flask up to 100ml.

Channel **D** contained ammonium acetate buffer solutions with different pH-values (3, 5, 7, 8); these buffers were prepared through dissolving 771mg ammonium acetate in 195ml of water and the following adjustment of the pH. Buffer pH 3 was prepared through addition of a 1:1 dilution of acetic acid with water, the same counts for the buffer solution for pH 5, but only a few drops of the acetic acid solution were necessary to adjust the pH.

The pH of the buffer solutions for pH 7 and pH 8 was adjusted to the relevant value through a few drops of a prepared 1:1 dilution of ammonium hydroxide with water. After the adjustment of the pH the respective solution was filled up with water to 200ml.

For the investigations of the chromatographic behaviour as well as the online-SPE of imiquimod, the contents of the mobile phase are listed in table 21.

Table 21: Contents of the mobile phases for imiquimod/HSA behaviour-studies.

Solv. channel	A	B	C	D
H ₂ O	100%	-	99.75%	100%
ACN	-	100%	-	-
TFA	-	-	0.25%	-
NH ₄ OAc	-	-	-	50mM *

*... pH-values adjusted to 3, 5, 7 or 8 (see above); for online-SPE of imiquimod adjusted to pH 8

3.3.5.4. Elution gradients

To evaluate the chromatographic behaviour of the standards (imiquimod 10ng/μl; HSA 100ng/μl), several eluent-gradients have been used; the first part comprised the isocratic elution of the standards from a RP-monolith. The standards were measured for each pH at varied isocratic contents of ACN (80, 60, 40, 20, and 0%)

The second part included the elution of the standard from a CX-monolith, applying two different pH-steps; in the first one the pH was decreased from 7 to 2 and the second one decreased from pH 8 to pH 2. These pH-gradients were measured at two different ACN contents (80% ACN and 0%). Table 22 lists the exact program for the applied pH-gradient for an ACN-content of 80%.

Table 22: Elution gradient imiquimod/HSA-investigations.

Time [min]	A [%]	B [%]	C [%]	D [%]
0-5	0*	80*	0	20
6-26	0*	80*	20	0
27-40	0*	80*	0	20

*... also measured at 100% A, 0% B

For the elution of imiquimod under SPE-conditions an optimised gradient (listed in table 23) has been applied: The mobile phase starts at a composition of 80% B and 20% D, this phase lasts for 1 minute. After this, the content of B is decreased within 0.1 minute to 20% and hold for 1 minute again. Then, the content of D is set to 0% and that of C to 20%, this change happens within 0.1 minutes. This composition is constant for 10 minutes, after this it changes in 0.1 minutes to 80% B again. After 1 further minute an anew change between solvent C and D is performed within 0.1 minutes, D increases to 20%, while C is set to 0%. This phase lasts for 10 minutes to condition the column.

Table 23: Optimised eluent-gradient for online-SPE of imiquimod.

Time [min]	A [%]	B [%]	C [%]	D [%]
0 – 1	0	80	0	20
1.1 – 2	60	20	0	20
2.1 – 12	60	20	20	0
12.1 – 13	0	80	20	0
13.1 – 22	0	80	0	20

4. Results & Discussion

Many studies for the preparation and characterisation of monolithic stationary phases utilizing ROMP have been published [2-5, 66-76]. Up to the present the influence of the terms of polymerisation as well as the functionalisation of ROMP-derived media on the material and chromatographic properties had been investigated for analytical columns [2, 3]. Further studies determined the impact of downscaling of the id of non-functional monolithic columns to morphology and therefore to separation performance [4, 5, 76]. The separation performance of miniaturised functional ROMP-derived monolithic media hasn't been investigated so far.

So in this work, the influence of different functionalisation techniques and conditions on the separation performance of functional monoliths derived by ROMP in cap-HPLC was evaluated. Therefore, monolithic columns with 200µm inner diameter for cation-exchange (CX) and anion-exchange (AX) chromatography have been investigated in their separation performance of a peptide standard (for CX) and an oligonucleotide standard (for AX). A further scope was the assessment of the applicability of functional capillary monoliths in clinical research, because of the possibility of cap-HPLC to handle very small sample volumes that often appear in medical-analytical fields. This applicability of CX-monolithic separation media was demonstrated through the online-SPE of imiquimod in human biofluids.

4.1. Chromatographic evaluation of CX monoliths

ROMP-derived CX monoliths functionalised with two grafting techniques at different conditions resulting in different ion exchange capacities have been provided. Their separation performance was investigated and the influence of the functionalisation parameter on the separation properties evaluated.

The chromatographic evaluation of the prepared monoliths was performed with a mixture of 4 synthetic peptides. These peptides differed mainly in their charge, which ranged from +1 to +4 but also in their hydrophobicity index, see table 24.

Table 24: Charge and hydrophobicity index used synthetic peptides.

Peptide No.	P1	P2	P3	P4
Charge	+1	+2	+3	+4
Hydrophobicity index	18.6	23.1	28.4	30.6

In order to evaluate the interaction of the analytes with the hydrophobic monolithic backbone the chromatographic behaviour of the analytes on RP-monoliths at varied pH-values (pH 7 and 2) was investigated. In all experiments, the peptides showed no interaction (elution in the injection peak) or were not possible to detect.

The effects of the changes of the functionalisation parameters and techniques to the separation performance were characterised chromatographically; following experiments have been performed:

- Optimisation of the chromatographic conditions
- Influence of the functionalisation parameters on the separation performance (determination of t_R , $w_{1/2}$, S and R)
- Evaluation of the hydrophobicity (measurements at ACN-contents of 40, 30, 20, 10 and 0 %)

4.1.1. Optimisation of chromatographic conditions

The prepared monoliths should differ in their separation properties – so it was necessary in the beginning to optimise the sample separation that this differences between the monoliths show up in the best possible way.

To minimise the influence of a potential hydrophobic interaction, it was preferable to use a high content of non-polar solvent – in this case ACN - in the mobile phase. On the other hand parts of the mobile phase also consist of salts, which are insoluble in ACN (sodium phosphates as buffer substances and NaCl as eluent). The maximum content of ACN with solubility for all components of the mobile phase was determined to 40%; the maximum concentration of NaCl was 0.5M in this case.

Also the content of phosphate buffer was investigated and optimised because there is a clear influence of the buffer concentration to the separation. High contents decreased the ionic interactions between analyte and stationary phase and shortened the retention times of P1 and P2 as shown in figure 10. It shows the decrease of the retention times (especially for P1 & P2) when the buffer concentration was increased from 1mM from 5mM to 10mM buffer . Higher concentrations led to elution of P1 & P2 in the injection peak and also less amount of buffer was not practicable, because of the fact that P4 wasn't possible to elute. Finally, the buffer-concentration was fixed to 1mM.

It has to be noted, that the used standard concentrations in the case of the optimisation of the buffer concentration was different to the further investigations, so the peak heights do not correlate with the further chromatograms.

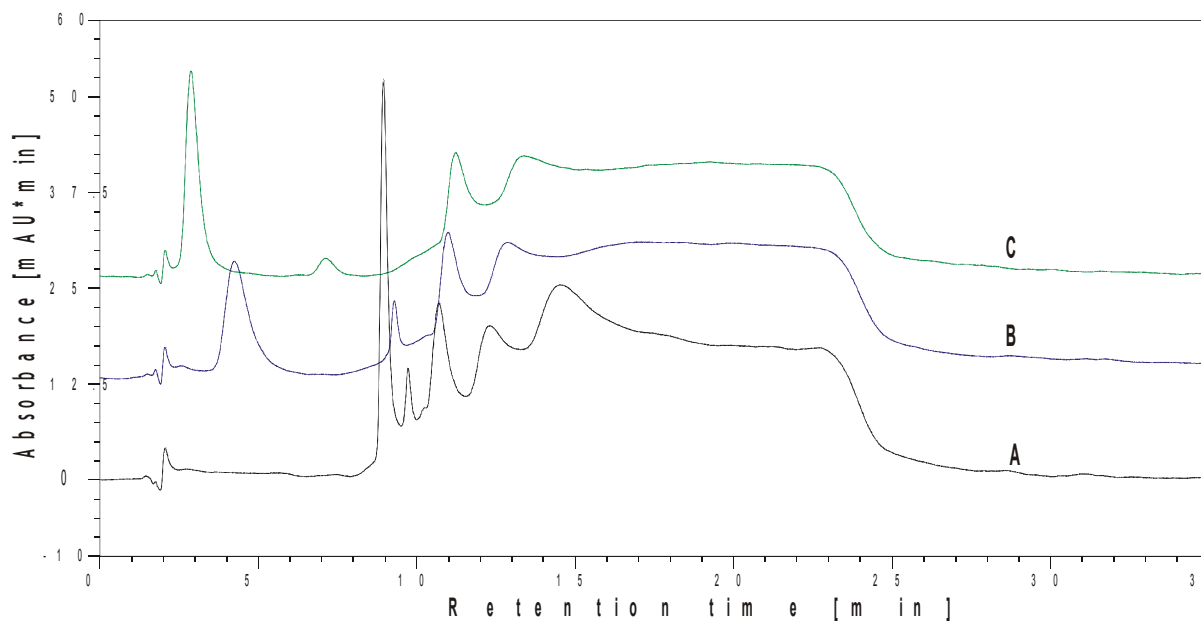


Figure 10: Separation performance depending on the buffer concentration: 1mM buffer (A), 5mM (B), 10mM (C).

Hence, the evaluation of the separation efficiency was performed at 40% ACN, 1mM buffer concentration and an elution-gradient of NaCl in a concentration from 0 to 0.5M. In experimental series with lower contents of ACN (alike the evaluation of hydrophobicity) the NaCl-concentration could be increased up to 0.76M; the slope of the NaCl-gradient was kept constant as a matter of course to still allow the comparison of the outcomes.

4.1.2. Influence of the functionalisation parameters on the separation performance

Following CX-monoliths have been investigated (monoliths see table 4):

- *In-situ* grafted monoliths, grafted at different temperatures (M1, M2)
- *Post-synthesis* grafted monolith (M3)

In general good ion-chromatographic performance was observed for all monoliths.

4.1.2.1. *In-situ*-grafting

As shown in figure 11, the stationary phase of M1 provides good separation of the described synthetic peptides; they elute in the order of their charges, first P1, then P2 followed by P3 and P4. Remarkable is that P1, the synthetic peptide with the lowest charge (+1) elutes in the injection peak. This means that the ionic interaction with the stationary phase is too weak, what may be due to the fact, that the present phosphate buffer has also a significant ionic strength, which decreases the forces between stationary phase and the analyte. P1 quasi gets eluted from the column through the content of buffer salts in the mobile phase. The peptides P2, P3 and P4 elute as expected in the NaCl-gradient (recognised by the step-up of the baseline). This shows that the main forces between analytes and stationary phase are of ionic nature.

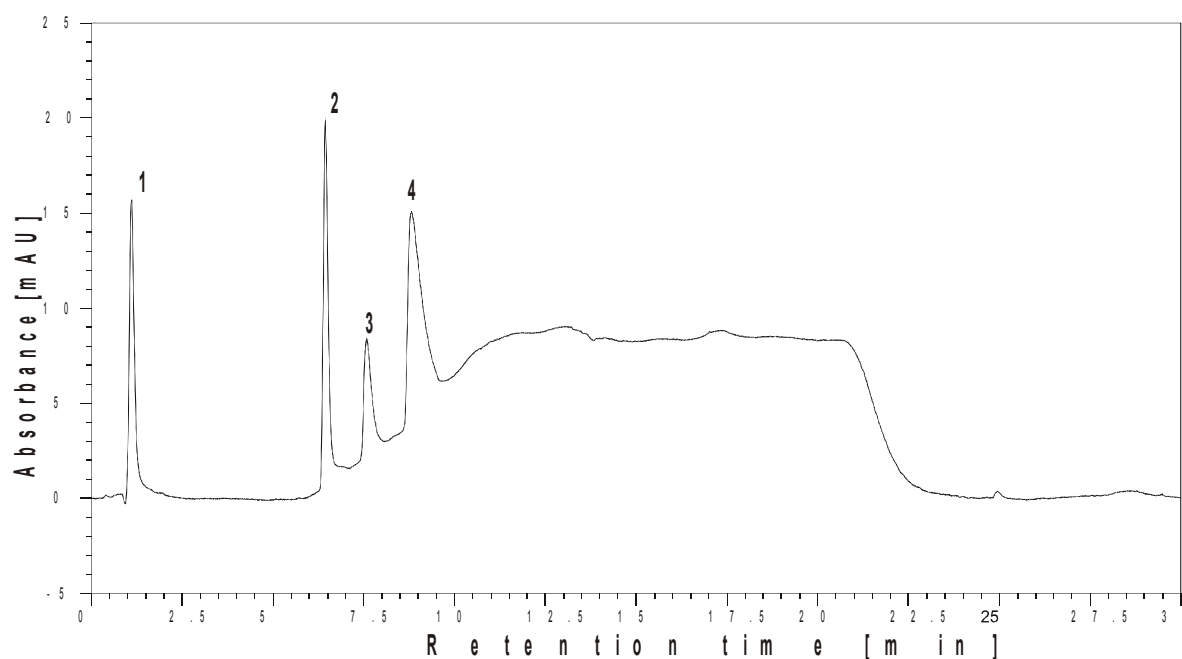


Figure 11: Peptide separation of M1 at 40% ACN.

Table 25 lists the evaluated values for t_R , $w_{1/2}$, S and R and their relative standard deviation (CV). It is observable that the peak widths increase the higher the charge of the analyte gets (in addition to “Eddy-diffusion”) while the symmetry is decreasing. This could be put down to the stronger interactions between analytes with high charges and the stationary phase.

The values for the resolution show baseline-separation of all peaks, P1 has because of its elution in the injection peak a clearly higher resolution than P2 and P3 which elute in the gradient. As a matter of fact, it's not possible to generate a value for the resolution of P4 because of the mathematical formula (see equation 10), that can't be calculated for the last peak, lacking a peak number X+1.

Table 25: Retention times (t_R), peak widths ($w_{1/2}$), peak symmetry (S) and resolution (R) for M1 at 40% ACN.

	t_R [min]	$w_{1/2}$ [min]	S	R
P1	1.11	0.15	0.9	20.75
	1.09	0.14	0.97	22.87
	1.08	0.12	0.88	21.91
Mean	1.09	0.14	0.92	21.84
Std-dev.	0.02	0.02	0.05	1.06
CV [%]	1.40	11.18	5.16	4.86
P2	6.25	0.14	1.55	3.45
	6.43	0.14	1.55	3.64
	6.34	0.16	1.51	3.63
Mean	6.34	0.15	1.54	3.57
Std-dev.	0.09	0.01	0.02	0.11
CV [%]	1.42	7.87	1.50	2.99
P3	7.38	0.24	1.78	2.09
	7.58	0.23	1.94	2.24
	7.56	0.23	2.09	2.11
Mean	7.51	0.23	1.94	2.15
Std-dev.	0.11	0.01	0.16	0.08
CV [%]	1.47	2.47	8.00	3.79
P4	8.73	0.52	3.92	
	8.81	0.42	2.74	
	8.69	0.4	3.33	
Mean	8.74	0.45	3.33	
Std-dev.	0.06	0.06	0.59	
CV [%]	0.70	14.39	17.72	

To evaluate if the different functionalisation temperature affects the separation performance of the stationary phase, the monolith M2 will be compared with the above mentioned monolith M1.

According to table 4 M2 shows a higher capacity than M1, what becomes noticeable in the difference of their separation performance, observable in figure 12. P1 shows no raise of its retention time, because it elutes in the injection peak for both monoliths. The retention times of the three synthetic peptides that elute in the

gradient (P2-P4) increase (values shown in table 26); though it's just a small difference, it's significant. The demonstrated increase of the retention times mirrors the expectations, that an higher amount of functional groups on the stationary phase leads the stronger interaction with the analyte and therefore to an longer residence-respectively retention time.

While the values of the peak widths as well as that of symmetry (also mentioned in table 26) show no significant changes, the resolution suggests a trend to higher values for M2 in comparison to M1. As it seems, the optimisation of the conditions for functionalisation benefits the separation performance of the stationary phase.

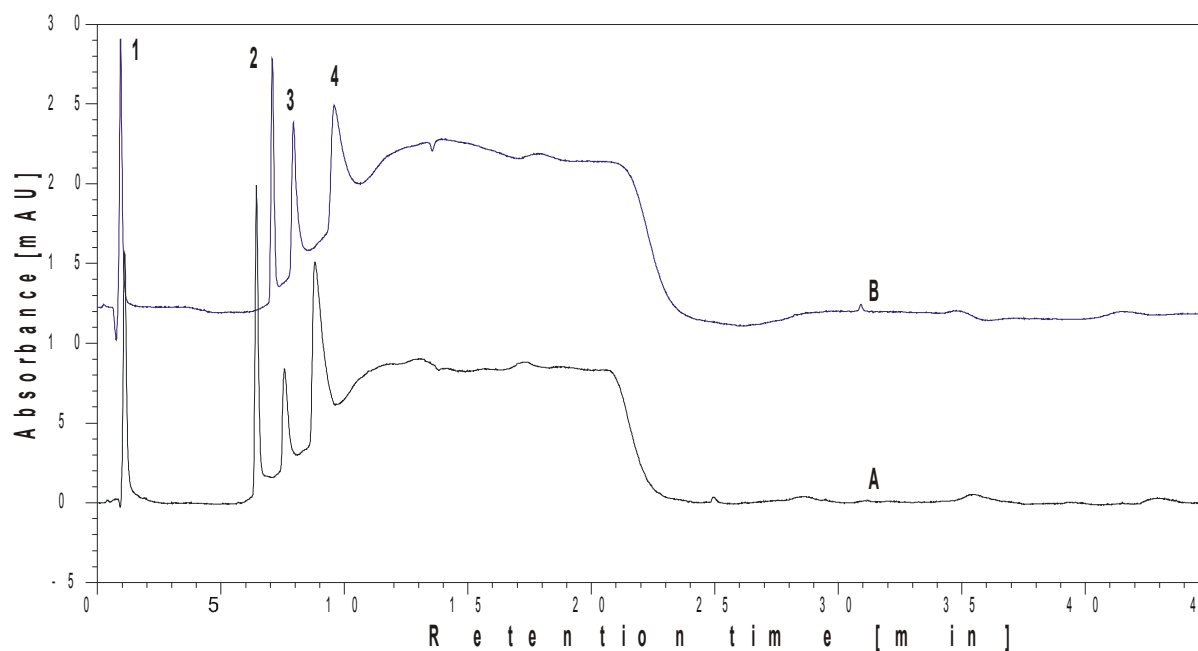


Figure 12: Peptide separation at 40% of M1 ACN (A) compared to M2 (B) .

Table 26: Retention times (t_R), peak widths ($w_{1/2}$), peak symmetry (S) and resolution (R) for M2 at 40% ACN.

	t_R [min]	$w_{1/2}$ [min]	S	R
P1	0.93	0.11	1.27	32.61
	0.91	0.11	1.31	30.49
	0.94	0.12	1.29	29.64
Mean	0.93	0.11	1.29	30.91
Std-dev.	0.02	0.01	0.02	1.53
CV [%]	1.65	5.09	1.55	4.95
P2	7.26	0.12	1.45	3.12
	6.81	0.12	1.27	3.24
	7.08	0.13	1.48	3.17
Mean	7.05	0.12	1.40	3.18
Std-dev.	0.23	0.01	0.11	0.06
CV [%]	3.21	4.68	8.11	1.90
P3	8.09	0.19	1.82	2.37
	7.65	0.18	1.86	2.84
	7.93	0.19	2.2	2.91
Mean	7.89	0.19	1.96	2.71
Std-dev.	0.22	0.01	0.21	0.29
CV [%]	2.82	3.09	10.65	10.85
P4	9.44	0.48	2.41	
	9.34	0.52	2.65	
	9.58	0.47	2.71	
Mean	9.45	0.49	2.59	
Std-dev.	0.12	0.03	0.16	
CV [%]	1.28	5.40	6.13	

4.1.2.2. Post-synthesis grafting

The CX-monolith M3, which was surface-modified via *post-synthesis* grafting, shows in comparison to M2 a clear difference in its separation performance. P1 again eluted in the injection peak and therefore also for M3 no difference of the values of P1 can be observed, respectively evaluated.

Below mentioned table 27 shows the restated increase of the retention times of the peptides 2 to 4, figure 13 the corresponding chromatograms. The increase of the retention times is significant trend for P2, P3 and P4; they have definitely increased retention times. A raise of the resolution, compared to M2, can be found, again because of the higher capacity which means more ionic groups on the monolithic surface and therefore an increased ionic interaction. Widths and symmetry of the peaks show no significant change – except of P4. It is necessary to mention the fact that P4 elutes in the isocratic area of the elution-gradient, so the increase of the

retention time appears larger, as it should be in the case of an extended raising area, which wasn't possible to achieve. As mentioned in section 4.1.1., a further increase of the content of NaCl was not practicable, because of its low solubility at the used mobile phase composite.

So symmetry and peak widths cannot be compared with the other monoliths because of this different gradient slope. This also affected the values of the retention times and the resolution.

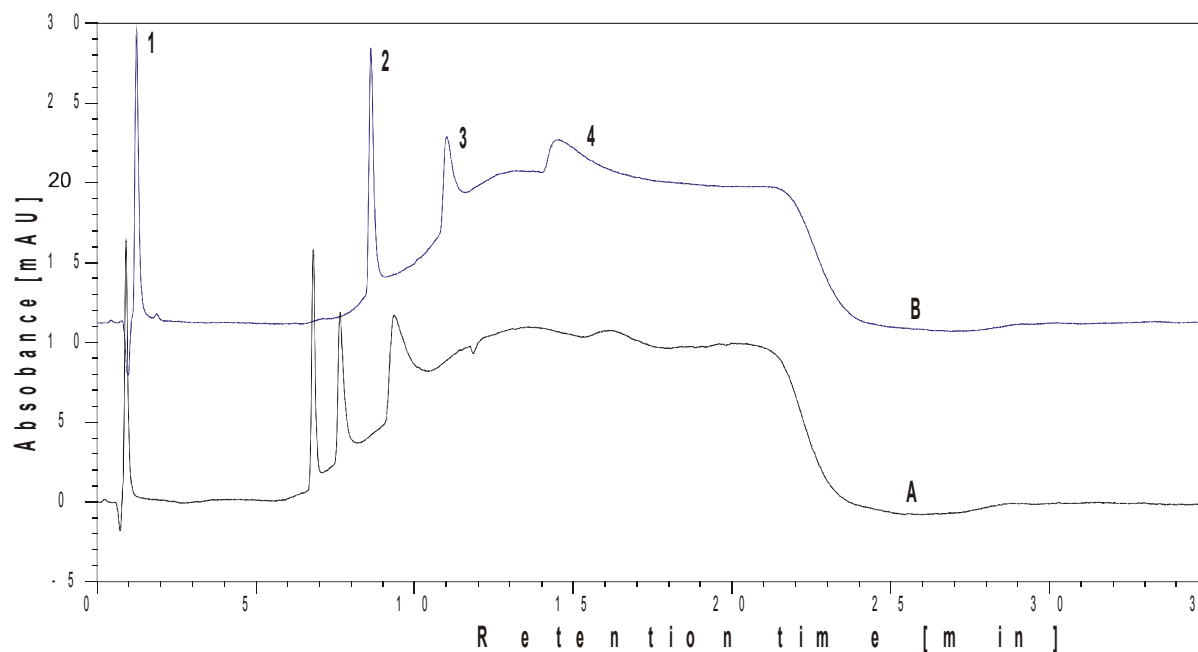


Figure 13: Peptide separation of M2 at 40% ACN (A) compared to M3 (B).

Table 27: Retention times (t_R), peak widths ($w_{1/2}$), peak symmetry (S) and resolution (R) for M3 at 40% ACN.

	t_R [min]	$w_{1/2}$ [min]	S	R
P1	1.22	0.11	1.47	33.33
	1.19	0.11	1.43	32.13
	1.17	0.12	1.46	32.84
Mean	1.19	0.11	1.45	32.77
Std-dev.	0.03	0.01	0.02	0.60
CV [%]	2.11	5.09	1.43	1.84
P2	8.54	0.15	1.72	6.38
	8.41	0.16	1.7	5.71
	8.53	0.15	1.72	5.72
Mean	8.49	0.15	1.71	5.94
Std-dev.	0.07	0.01	0.01	0.38
CV [%]	0.85	3.77	0.67	6.47
P3	10.87	0.28	2.31	3.13
	10.69	0.32	2.32	3.35
	10.72	0.3	2.27	3.17
Mean	10.76	0.30	2.30	3.22
Std-dev.	0.10	0.02	0.03	0.12
CV [%]	0.90	6.67	1.15	3.64
P4	13.84	0.84	2.7	
	13.59	0.7	1.96	
	13.41	0.7	2.41	
Mean	13.61	0.75	2.36	
Std-dev.	0.22	0.08	0.37	
CV [%]	1.28	5.40	6.13	

Figure 14 shows the increase of the retention times for the monoliths with higher capacity, the little standard deviations stand for the good reproducibility of the experiments.

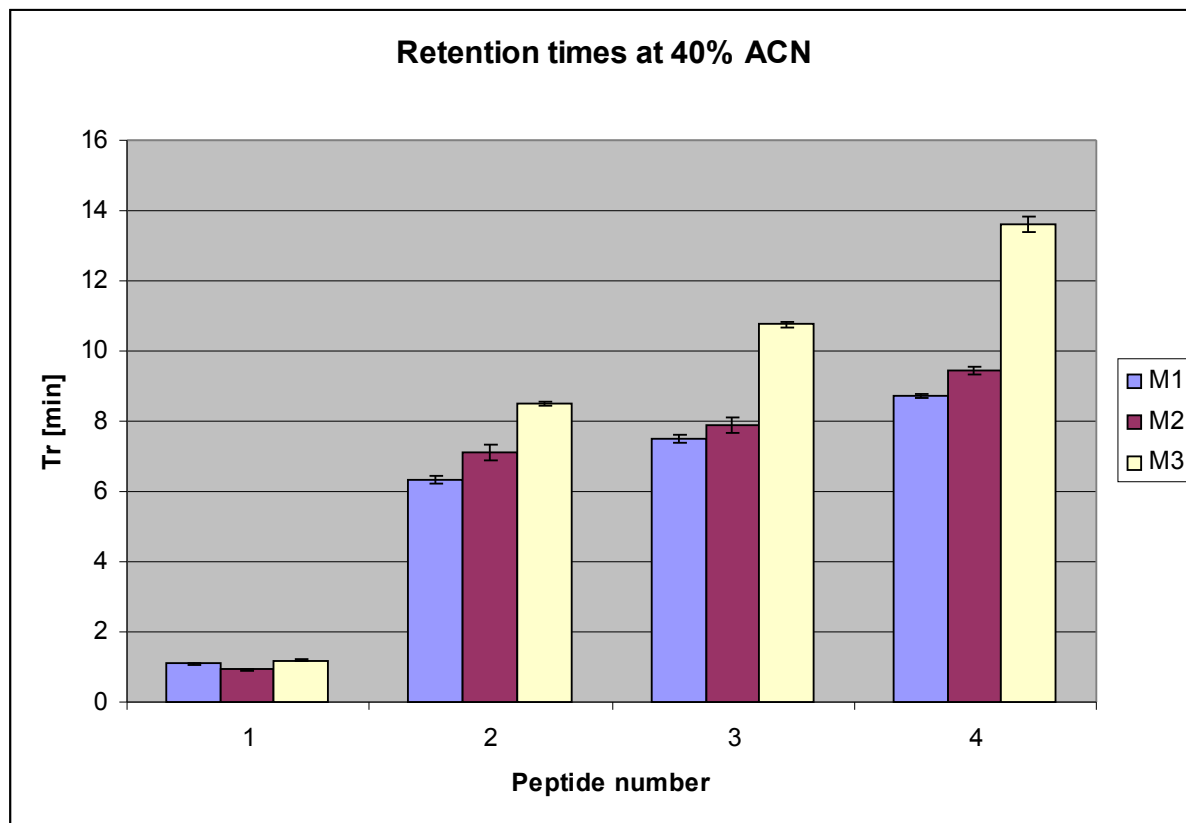


Figure 14: Comparison of t_R at 40% ACN of M1 – M3.

4.1.3. Evaluation of hydrophobicity

As in section 3.1. described, the stationary phases of the monoliths were prepared using NBE and DMN-H₆. Therefore it was presumably, that besides ionic interactions there will be hydrophobic forces between stationary phase and analytes. A decrease of the amount of the non-polar solvent ACN in the mobile phase should mean an increase of the hydrophobic forces between analyte and stationary phase. This would show up in an enlargement of the retention times that would be so much the greater, the stronger the hydrophobic character of the used stationary phase.

So to assess the strength of the hydrophobic interaction, the ACN-content of the mobile phase was decreased successive from 40-0%; the influence to the separation performance was investigated.

First, the two *in-situ* grafted monoliths have been investigated; because both show almost the same behaviour, only M2 will be discussed here.

Figure 15 shows the comparison of the separation performance of M2 at 40% ACN as well as at 30% ACN. At 40% the peptides elute well separated in order of their charge, P1 in the injection peak, P2-P4 in the elution gradient. As observable, the retention times as well as the distances between the peaks in the gradient (P2 - P4) increase when the ACN-content is lowered to 30% ACN. At an ACN-rate of 10% also P1 eluted in the NaCl-gradient and P3 and P4 remained on column. In the absence of ACN all peptides were not possible to elute. This result admits the conclusion, that the hydrophobic interaction of the analytes with the stationary phase is the reason for this increasing of the retention times, the partial hydrophobic character of the separation media shows up clearly. A content of 40% ACN perhaps didn't inhibit the hydrophobic interaction completely, but as mentioned, the ACN-amount couldn't be further raised because of the bordered solubility of the salts.

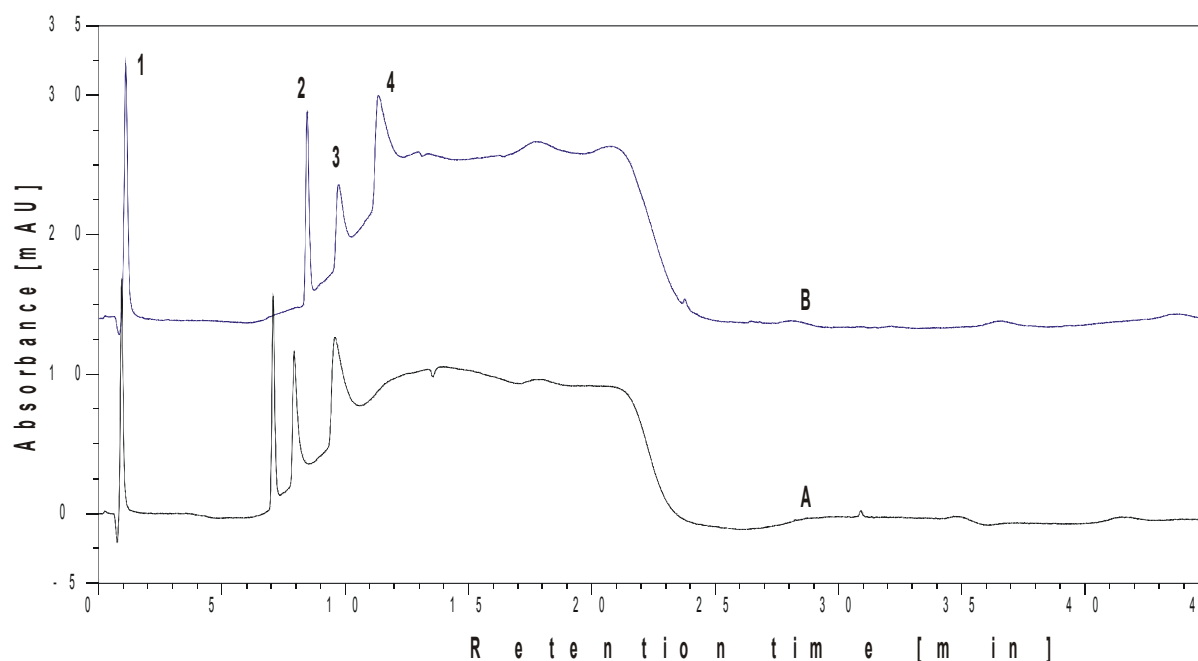


Figure 15: Assessment hydrophobicity of M2; 40% ACN (A), 30% ACN (B).

The post-synthesis grafted monolith M3 shows contrary to M1 and M2 no significant change of the retention times when the ACN-content is decreased from 40% to 30% (see figure 16). This result indicates that this monolith shows up a lower hydrophobicity than the former, what seems quite reasonable on closer examination.

Because of the anew addition of initiator before the actual functionalisation more parts of the polar polymer-backbone are prepared for the following modification, not only the active ends of the polymer chains. So during functionalisation not only more functional monomer is fixed on the polymer surface, but also the hydrophobic character of the backbone will be „shielded“ from the chromatographic surroundings through this functional groups.

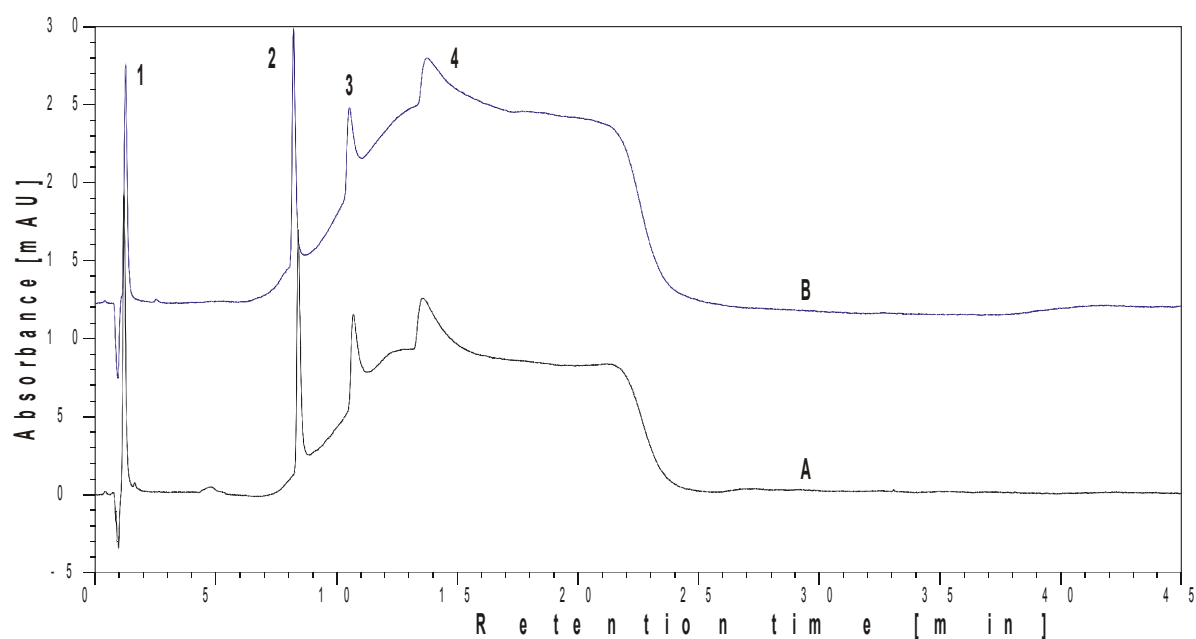


Figure 16: Assessment hydrophobicity of M3; 40% ACN (A), 30% ACN (B).

4.2. Chromatographic evaluation of AX-monoliths

ROMP-derived AX-monoliths functionalised with two grafting techniques and different conditions resulting in different ion exchange capacities have been provided. Their separation performance was investigated and the influence of the functionalisation parameter on the separation properties evaluated.

The chromatographic evaluation of the provided AX-monoliths was performed with a mixture of poly-oligothymidines ($d(pT)_{12-18}$). These differed in the number of thymidines which reached from 12 to 18 and therefore also showed higher values of their charge with increasing length respectively molecular weight.

Experiments to investigate the chromatographic behaviour of the analytes on RP-monoliths at pH 7 and pH 2 showed only little interaction of the oligonucleotide standard with the stationary phase at pH 7, figure 14 shows the separation performance of a RP-monolith at pH 7, applying an ACN-gradient from 0-80%. It is observable that the oligonucleotides elute at the beginning of the gradient, a separation wasn't possible to achieve.

To evaluate the effect of the different functionalisation parameter, following experiments have been performed:

- Optimisation of the chromatographic conditions
- Influence of the functionalisation parameters on the separation performance (determination of t_R , $w_{1/2}$, S and R)
- Evaluation of the hydrophobicity (measurements at ACN-contents of 30, 25, 20, 15, 10, 5 and 0 %)

4.2.1. Optimisation of the separation conditions

As already described for CX-monoliths, also here in the beginning the chromatographic conditions have been optimised to show the differences of the separation performance of the prepared monoliths in the best possible way and to avoid problems that appeared in CX evaluation through the use of salt gradients.

The optimisation of the buffer concentration is shown in figure 17, it shows the separation at buffer concentrations of 20mM and 5mM, and as observable the separation containing 20mM buffer in the mobile phase features shorter retention times and higher resolution, especially for the nucleotides p(T)₁₂₋₁₄. But further measurements showed that this high concentration of buffer salts led to problems in the mixing valve, where all contents of the mobile phase are mixed together. For high ACN-contents and high buffer concentrations it was possible that some buffer-salt precipitated because of local solvent inhomogeneities in the mixing unit.

Because of this, the separation was performed at a buffer concentration of 5mM and - compared to the CX measurements - a decreased ACN-content of 30%. So it is necessary to mention the fact that the hydrophobic interaction between analytes and stationary phase is "less minimised" compared to CX-evaluation.

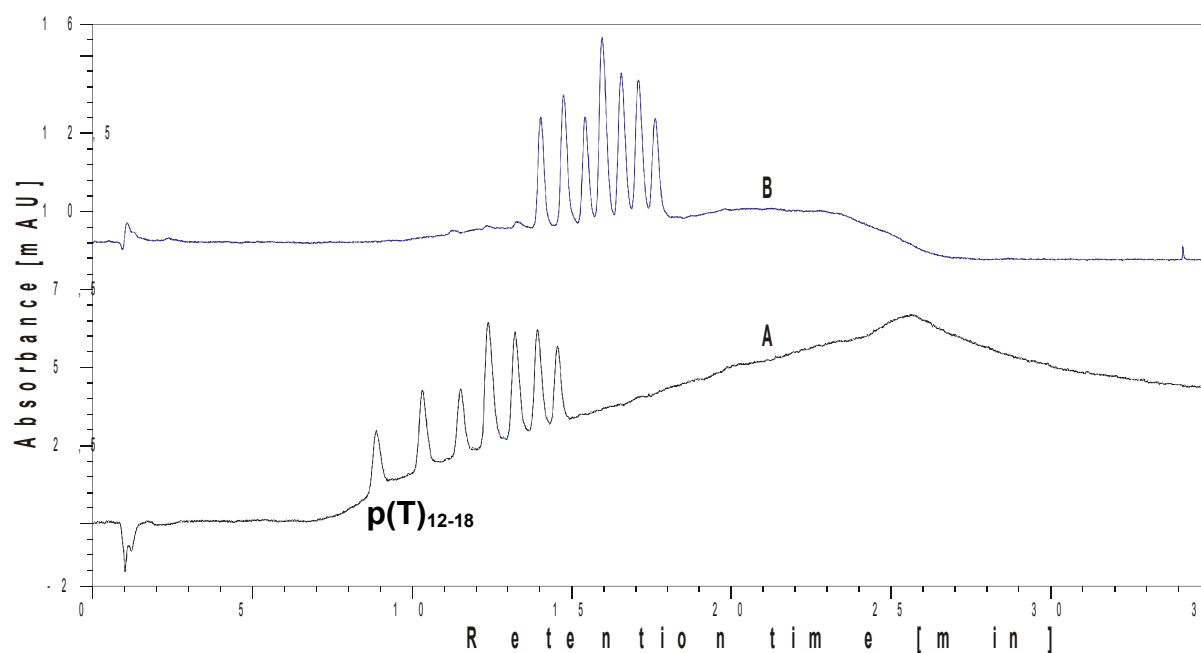


Figure 17: Separation performance at 20mM (A) and 5mM buffer concentration (B).

Also optimised was the concentration of sodium chloride in the elution gradient reached from 0-0.5M NaCl, the maximum concentration wasn't applied for most of the monoliths to shorten the time of conditioning. Only for the AX monoliths M8 and M9 it was necessary to extend the elution-gradient up to the mentioned NaCl-concentration of 0.5M to elute the analytes, all other experiments were performed with a maximum NaCl-concentration of 0.33M. Of course, the slope was the same for both gradients.

To achieve a good separation of the oligonucleotides, several elution-gradients of NaCl have been tested; the results for three of them are shown in figure 18. The separation performance changes for the better when the gradient slopes are decreased from 100mM/min to 15mM/min decreasing. While the standard isn't separated for the gradients A and B with a slope of 100mM/min respective 50mM/min, gradient C is able to separate the analytes in a good resolution. A further decrease of the slope wasn't practicable because of problems with the reproducibility on the part of the mixing unit.

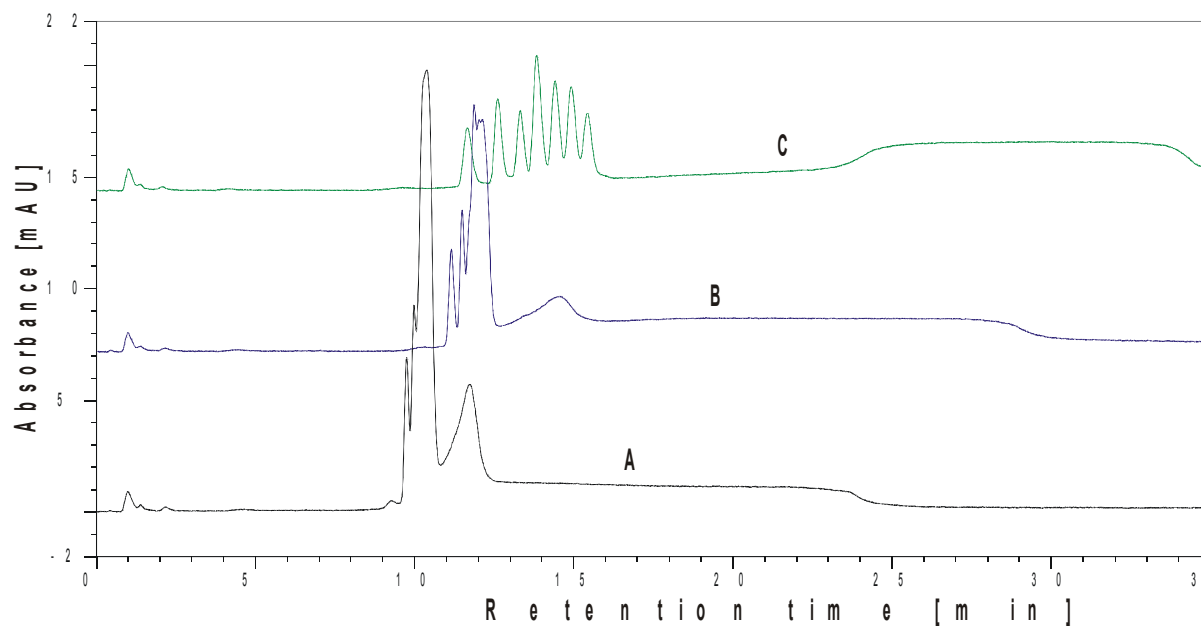


Figure 18: Elution-gradients; Gradient slope NaCl 100mM/min (A), 50mM/min (B), 15mM/min (C).

Influence of the functionalisation parameter on the separation performance

Following AX-monoliths have been investigated (used monoliths see table 5):

- *In-situ* grafted monoliths, grafted with different amount of NBE in the grafting mixture (M4, M5)
- *Post-synthesis* grafted-monoliths, grafted at different temperatures (M6, M7, M8, M9)
- *Post-synthesis* grafted-monoliths, grafted using different catalysts (M8, M9)

These investigations were carried out at an ACN-content of 30%.

4.2.2.1. *In-situ* grafting

In-situ grafted monoliths have been prepared and functionalised with different amounts of NBE added to the functionalisation mixture as investigated functionalisation parameter.

The separation performance of M4 and M5 was investigated at 15% ACN because of the fact, that at 30% ACN both monoliths were not able to separate the standard. Figure 19 shows the separation performance for M4 and M5 at 15%. It is observable that M4 doesn't separate the standard, the oligonucleotides elute in a broad peak within the gradient. M5 features a better separation performance, the analytes elute moderately separated. This enhanced performance is explainable through the higher capacity of M5; it leads to stronger interaction between stationary phase and the oligonucleotides.

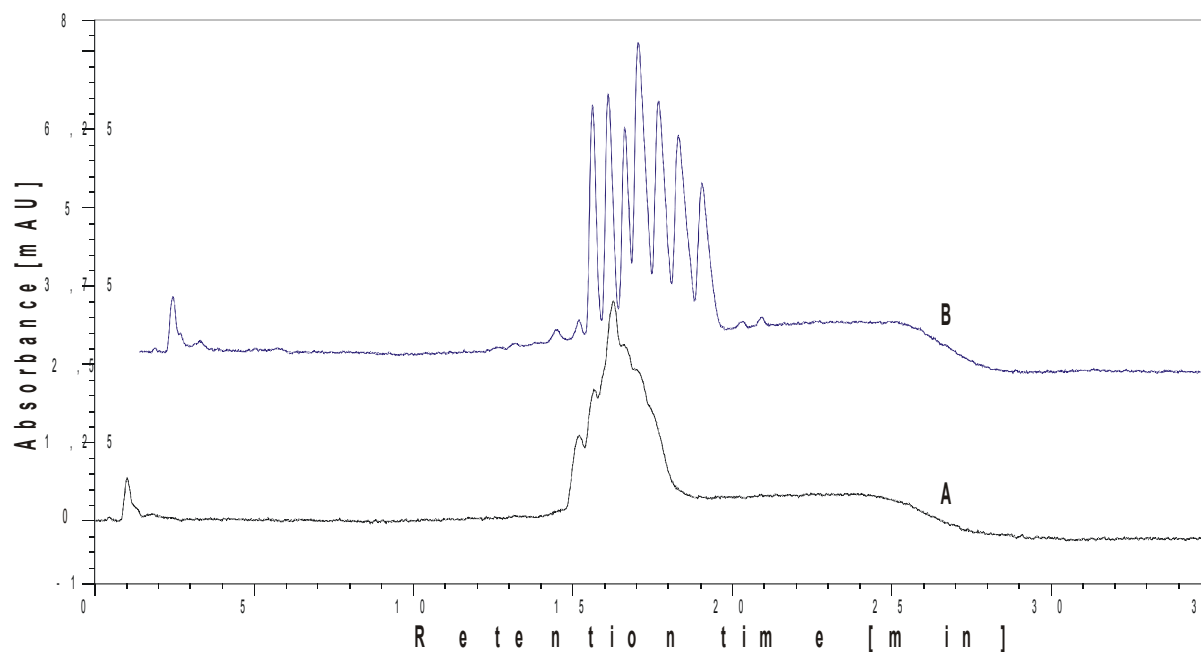


Figure 19: Separation performance at 15% ACN for M4 (A) and M5 (B).

4.2.2.2. Post-synthesis grafting

For *post-synthesis* monoliths two functionalisation parameter have been investigated. The first one was the temperature while *post-synthesis* grafting, the second one the used catalyst for grafting. The investigated temperatures were RT and 60°C, the catalysts Grubbs 1st generation and Hoveyda-Grubbs 2nd generation.

The influence of the grafting temperature was investigated through the comparison of M6, which was grafted at RT and M7, grafted at 60°C. In figure 20 it is observable, that M6 isn't able to separate the oligonucleotides, they elute again in a broad peak within the gradient. The separation performance of M8 is clearly better. All analytes elute well separated from each other in very good resolution. The higher capacity of M7 again leads to a better separation performance.

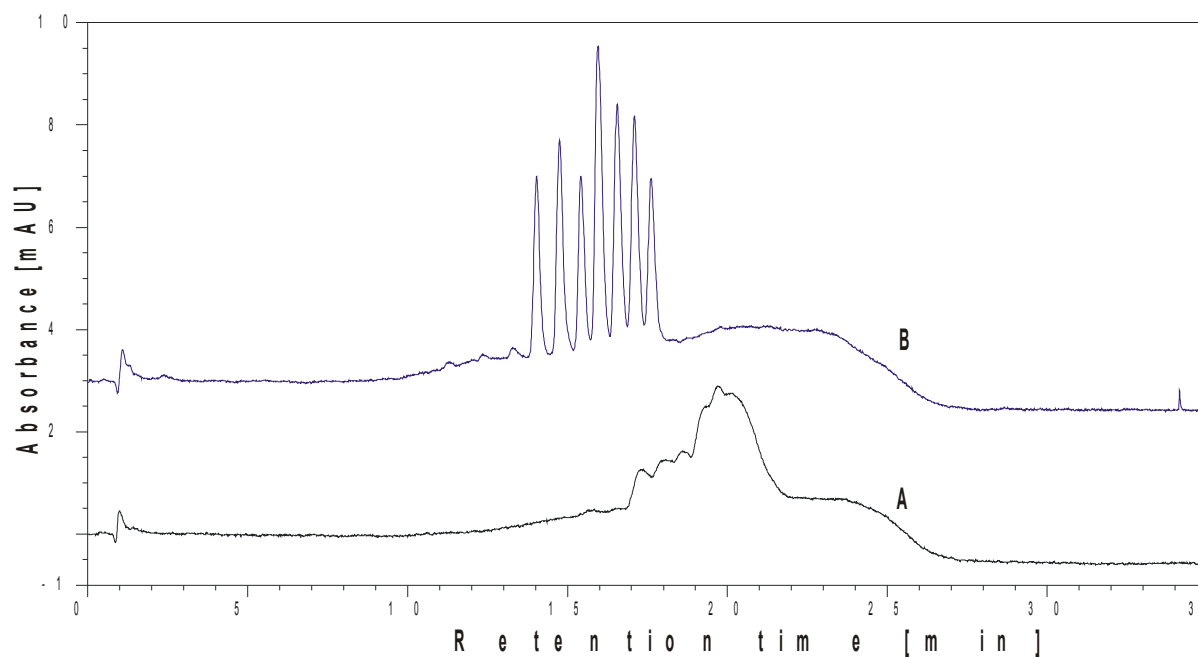


Figure 20: Separation performance of M6 (A) and M7 (B) at 30% ACN.

Figure 21 shows that the same counts for the monolith prepared with the grafting-catalyst 2nd Grubbs-Hoveyda. M8 doesn't fully separate the standard-oligonucleotides; the single oligonucleotides are identifiable, but their peaks are broad and overlap. M9 has a much better separation performance, all analytes elute well resolved. Note that the elution gradient has been risen up to a maximum NaCl-concentration 0.5M for both monoliths. The higher temperature while grafting seems to affect both capacity and separation performance in a positive way.

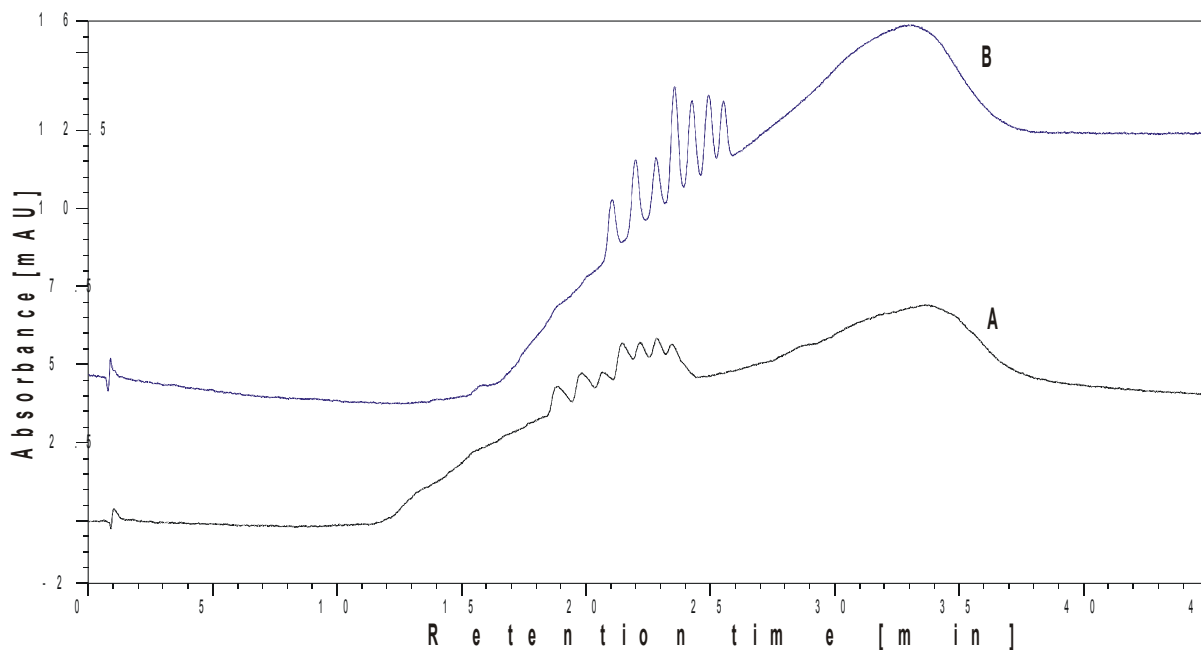


Figure 21: Separation performance of M8 (A) and M9 (B) at 30% ACN.

The influence of the grafting catalyst was evaluated through the comparison of M7 (grafting catalyst 1st Grubbs) and M9 (grafting catalyst 2nd Hoveyda). Their separation performance (see figure 22) shows, that both monoliths separate the standard very well. Remarkable is, that although M9 features an almost 4 times higher capacity, M7 possesses significantly better separation properties (see table 28, this evaluation also is exemplarily for the not mentioned values of the other monoliths).

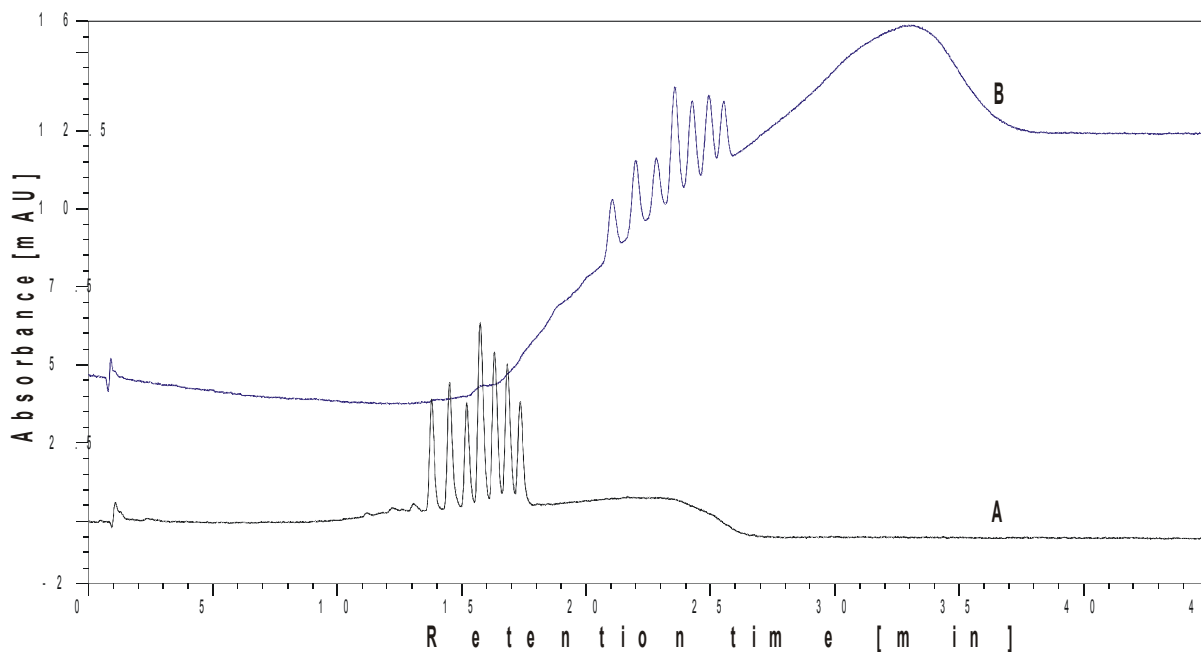


Figure 22: Separation performance of M7 (A) compared to M9 (B) at 30% ACN.

Table 28: Separation parameter of M7 compared to M9 at 30% ACN.

Analyte	M7			M9		
	t_R	$w_{1/2}$	R	t_R	$w_{1/2}$	R
p(T)₁₂						
Mean	14.04	0.20	2.07	20.58	0.34	1.57
CV [%]	1.8	0.0	2.4	1.2	2.9	2.9
p(T)₁₃						
Mean	14.76	0.21	1.91	21.50	0.35	1.45
CV [%]	1.8	0.0	3.1	1.3	2.9	0.7
p(T)₁₄						
Mean	15.45	0.21	1.41	22.35	0.35	1.22
CV [%]	1.7	2.7	1.4	1.2	3.3	2.5
p(T)₁₅						
Mean	15.98	0.24	1.44	23.04	0.33	1.21
CV [%]	1.5	0.0	0.8	1.1	3.0	1.9
p(T)₁₆						
Mean	16.56	0.23	1.33	23.71	0.33	1.11
CV [%]	1.5	4.3	1.6	1.0	1.7	1.9
p(T)₁₇						
Mean	17.08	0.23	1.32	24.34	0.33	1.06
CV [%]	1.4	2.5	1.9	1.0	3.5	2.9
p(T)₁₈						
Mean	17.35	0.22		24.93	0.32	
CV [%]	0.2	0.0		1.0	1.8	

The investigations show the clear influence of the functionalisation parameter on the separation performance of the monoliths; some of the AX-monoliths possess very good separation properties. But although the capacity has a positive effect on the performance, M7, which didn't feature the highest capacity, performed the best separation properties of the evaluated monoliths. This leads to the conclusion, that the capacity is just a guide value to assess the properties of the provided AX-columns, not the exclusive determining factor.

4.2.3. Evaluation of the hydrophobicity

To estimate the hydrophobic character of the different monoliths, again the content of ACN in the mobile phase was varied; contents from 30-0% were evaluated. A decrease of the amount of ACN should mean an increase of the hydrophobic forces between analyte and stationary phase. This would show up in an enlargement of the retention times that would so much the greater, the stronger the hydrophobic character of the used stationary phase. Therefore, the prepared monoliths have been measured at ACN-contents of 30, 25, 20, 15, 10, 5 and 0%. It can be told in the beginning, that at 5 and 0% ACN none the standard oligonucleotides was possible to elute for all measured monoliths, because of the heightened hydrophobic forces which also means, that all monoliths showed up a more or less strong hydrophobic character. It also has to be mentioned, that it was difficult to evaluate the changes of hydrophobicity because of the fact, that various factors influenced the evaluation.

First, not all monoliths separated the standard, so for some monoliths no retention times were evaluable. Second, the analytes did not all feature the same hydrophobicity (the longer the oligonucleotide, the higher its hydrophobicity) and third; the investigated analytes didn't elute always within the slope of the gradient over the whole investigated ACN-range; and only within the gradient measured retention times were comparable. Furthermore, the gradient delay time wasn't the same for all monoliths because of the different master pump flow.

4.2.3.1. In-situ grafting

Chromatograms of M4 aren't shown because of the lack of a standard-separation.

For M5 it is observable in figure 23, that already at a content of 30% ACN in the mobile phase most of the standard-analytes elute poorly separated in the NaCl-gradient and only short before it the two analytes with the lowest charges, pT₁₂ and pT₁₃. From 25% ACN on, all oligonucleotides elute in the gradient; moderately separated.

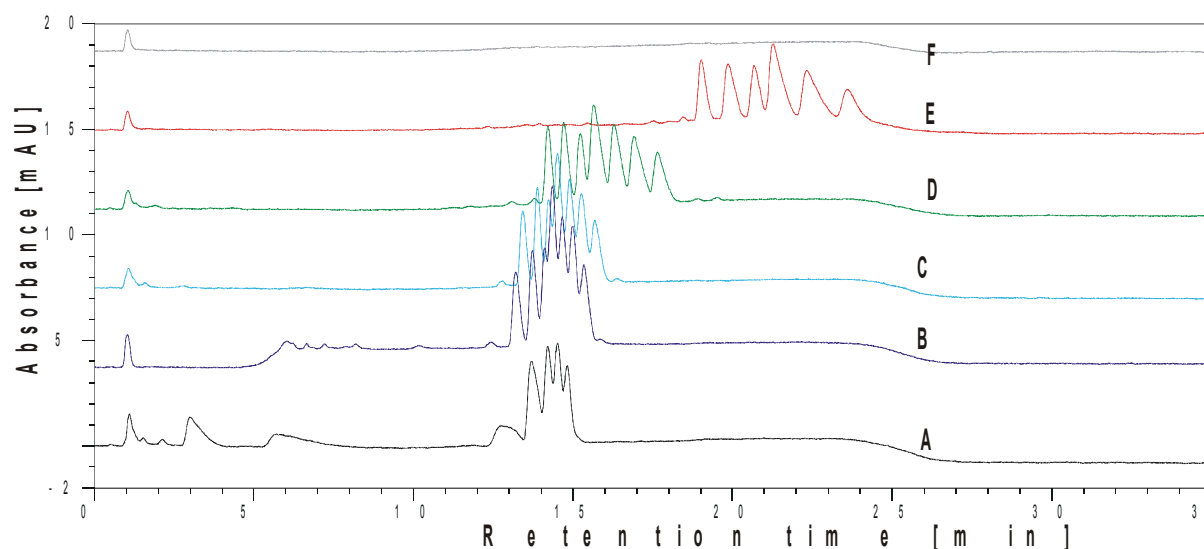


Figure 23: Chromatograms for M5 at different ACN-contents; 30% ACN (A); 25% ACN (B); 20% ACN (C); 15% ACN (D); 10% ACN (E).

4.2.3.2. Post-synthesis grafting

M6 also isn't mentioned because of the fact, that the analytes weren't separated.

Figure 24 shows that M7 separates the standard from 30 to 15% ACN very well, the retention times increase continuously with decreasing amounts of ACN. Beginning with 10% ACN four analytes start to remain on column. Also in this case the hydrophobicity of the column is clearly observable.

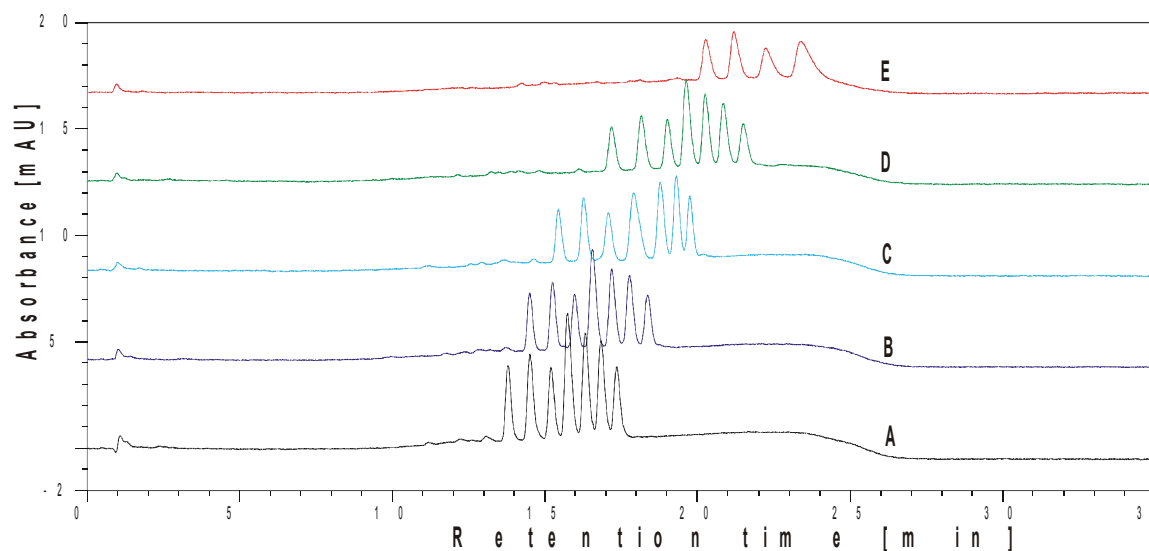


Figure 24: Separation performance for M7 at decreasing ACN-contents; 30% ACN (A); 25% ACN (B); 20% ACN (C); 15% ACN (D); 10% ACN (E).

M9 also separates the oligonucleotides from 30 to 15% ACN-content well resolved. The retention times increase slightly when the ACN-content is decreased. At 10% ACN the analyte with the highest hydrophobicity doesn't elute any more, this can be seen in figure 25. Also this monolithic possesses a clearly observable hydrophobic character.

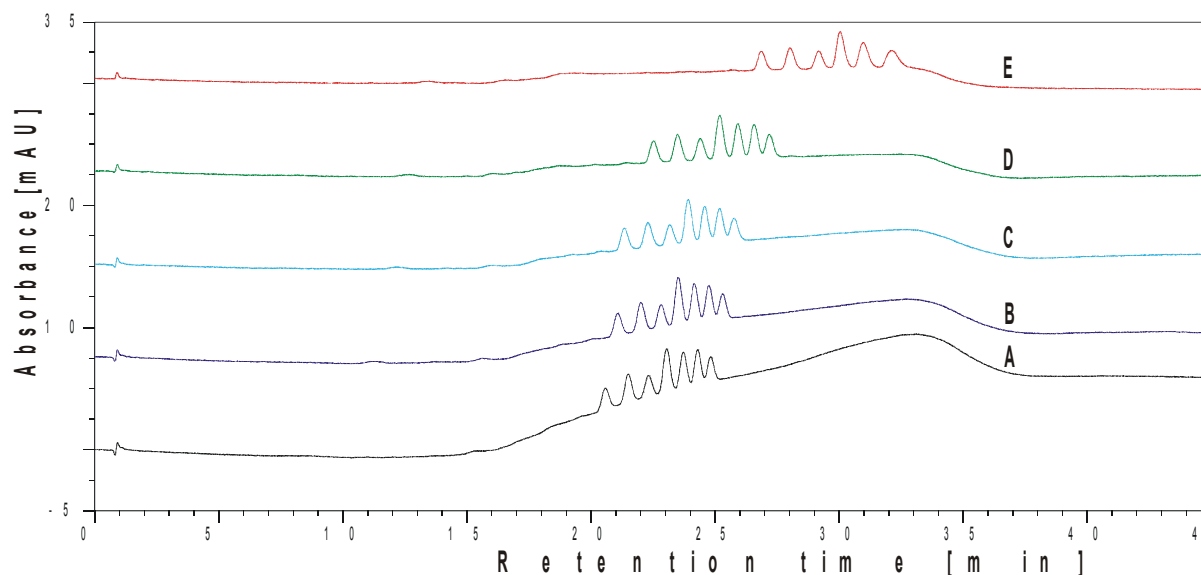


Figure 25: Separation performance for M9 at decreasing ACN-contents; 30% ACN (A); 25% ACN (B); 20% ACN (C); 15% ACN (D); 10% ACN (E).

When the separation performance of M7 (see. figure 24) and M9 are compared with each other, it is investigable, that with decreasing amount of ACN the retention times of M9 don't increase that much as they do for M7. This leads to the conclusion, that M9 is less hydrophobic than M7. This seems plausible, because of the higher capacity of M9. More capacity stands for more grafted functional monomer, so the onto the monolithic backbone grafted "tentacles" should be longer because of the higher polymerisation activity of the used catalyst. These longer tentacles can better "shield" the monolithic backbone from the surrounding than short ones.

To demonstrate the increase of the retention times more clearly, table 29 lists them for the oligonucleotide pT₁₂ when lowering the ACN-content from 25 to 20% and from 20 to 15%.

Table 29: t_R – increase (pT₁₂) of M7 and M9 at ACN-content – decrease.

ACN-decrease	T _R – increase M7	T _R – increase M9
25% - 20%	0.87	0.24
20% - 15%	1.74	1.19

4.4. CX-monoliths for online-SPE of imiquimod

The applicability of ROMP-derived ion exchange monoliths in medical research should be assessed. Cap-HPLC features advantages for some analytical questions in clinical research. It needs only very small sample volumes; this often appears in clinical analytics. In dermatology, for instance, small sample amounts are often obtained through open-flow microperfusion ^[77], the sample matrix in this case is ISF and only few of it can be gained out of the tissue. Second, cap-HPLC features high sensitivity and an increased mechanical stability. And third, it can be easily coupled with mass spectrometers because the applied low flow rates make the splitting of the eluate unnecessary.

Till now, the monoliths were applied as analytical columns, but the observed hydrophobic character of the provided monoliths suggests the use in online-SPE, which means the application of the ion exchange monoliths to separate the analytes of interest from the matrix and/or concentrate these analytes on-column.

Because all of this points, an application of the monoliths for dermal applied drugs was chosen. A potential analyte in dermatological research is the drug imiquimod.

Imiquimod ^[78] is the active ingredient of a patient-applied cream (trade name Aldara[®]) used to treat certain diseases of the skin, including skin cancers (basal cell carcinoma, Bowen's disease, superficial squamous cell carcinoma, superficial malignant melanomas, and actinic keratosis) as well as genital warts. It has also been tested for treatment of molluscum contagiosum and vaginal intraepithelial neoplasia.

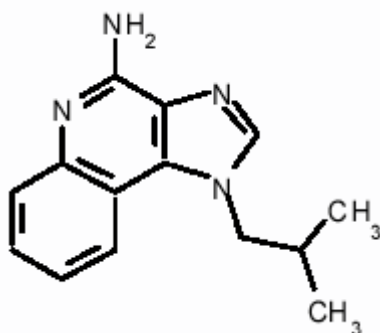


Figure 26: Structure of imiquimod.

Because imiquimod is differently applied from each patient, different doses are the consequence. Furthermore, there is little consensus about the necessary dose respectively the amount that insists the tissue and less literature regarding its analysis [79 - 81]. Therefore imiquimod was chosen as analyte for the following investigations; the sample matrix in which imiquimod appears is ISF, it consists of lots of body's own substances, mainly proteins such as human serum albumin (HSA) – so the monoliths were applied as SPE-columns to get rid of these impurities.

4.4.1. Method development for online-SPE of imiquimod with CX-monoliths

In order to separate imiquimod from HSA, the main component of ISF, the chromatographic behaviour of both substances has been investigated. The observations were made on a RP-monolith as well as a CX-column.

The performed experiments for the RP-investigations included the isocratic elution of imiquimod and HSA at

- different pH-values (pH 2 to 8)
- and different contents of ACN (0-80%)

The behaviour of imiquimod on RP-monoliths showed, that imiquimod didn't interact with the stationary phase, it eluted in the injection peak for all investigated pH-values and also percentages of ACN in the mobile phase.

HSA showed a chromatographic behaviour, that didn't differ with changes in the pH, but with the ACN-content. At low amounts of ACN in the mobile phase (0-40%), it remained longer on column than for higher contents (60-80%).

The performed experiments for CX-investigations comprised the elution of imiquimod and HSA through a gradient containing a pH-step from a higher "loading" pH-value to a low elution pH-value of pH 2.

This gradient has been varied in the following parameter:

- different loading pH (pH 7 and 8)
- different isocratic contents of ACN (0% and 80%)

The result of the investigations of the behaviour of imiquimod on CX columns was, that it elutes only when the pH decreases to 2, regardless of the ACN-percentage. The loading pH didn't influence the elution of imiquimod, so it was set to 8, because the higher the pH-value gets the more active are the CX-groups of the monolith which means stronger interaction with imiquimod.

The investigation of the chromatographic behaviour of HSA showed that most of it eluted at 80% of ACN already at a pH of 7 or 8, but note the fact, that a small amount still remained on column. Only at 80% ACN and pH 2 all HSA eluted. At 0% ACN HSA remained on the CX-column, independent of the pH.

Figure 27 shows the chromatograms for imiquimod and HSA when eluted through a pH-step from 8 to 2 and an isocratic content of 80% ACN, it is observable that most of the HSA elutes with the injection peak (1a) but unfortunately, also some HSA (1b) elutes almost at the same time as imiquimod (2).

1a

1b

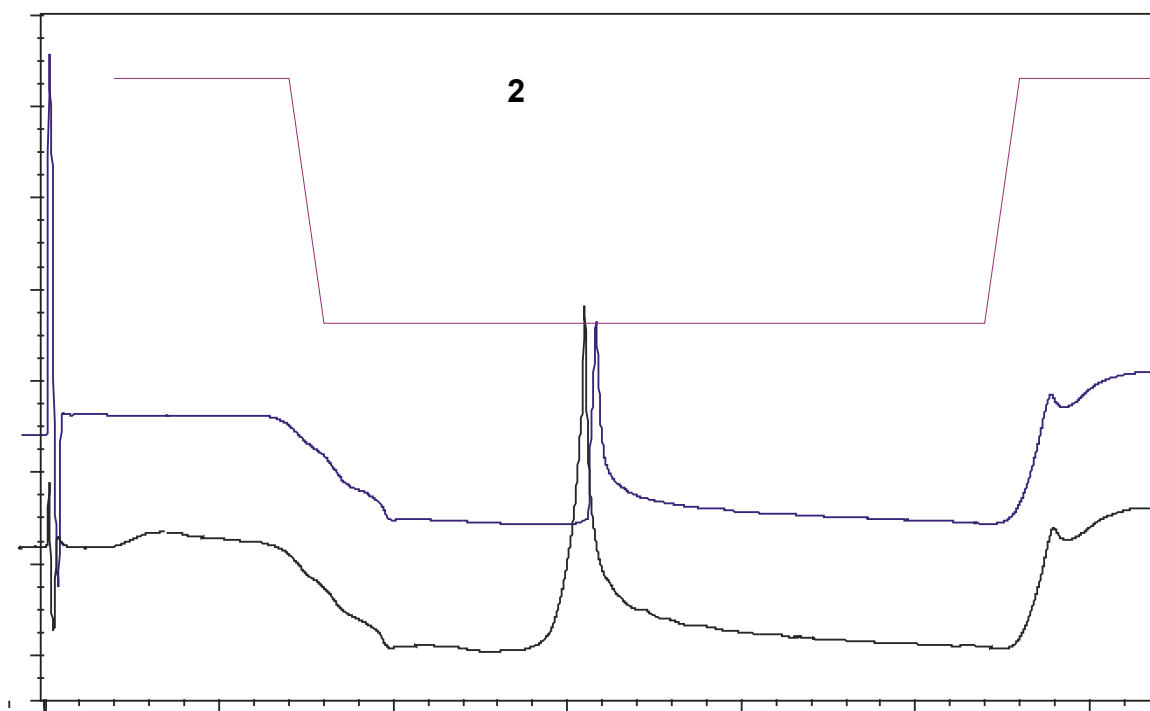


Figure 27: Elution of imiquimod (A) and HSA (B) through pH-step 8-2 at 80% ACN.

To prevent the simultaneous elution of HSA, a step with a lower ACN-content was inserted in the gradient, because of the fact that HSA didn't elute at this conditions. Figure 28 shows the chromatograms with an inserted step of 20% ACN at pH8. At the beginning of the gradient, the sample is loaded on column whereas most of the HSA already passes (1a); imiquimod is kept on the column. Then the content of ACN is decreased to 20% to keep the remaining HSA on-column. After that, the pH-value is changed to 2 to elute imiquimod (2) and thereafter the ACN-content is increased again to 80% at pH 2 to elute the remaining HSA (1b). Finally, the pH was set to 8 again to condition the column.

It is observable that HSA no longer elutes at the same time imiquimod does, the hydrophobicity of the CX-monoliths keeps the HSA on column; without this hydrophobic character this separation couldn't be performed. Note, that the inserted gradient step with low content of ACN also clearly sharpened the imiquimod-peak.

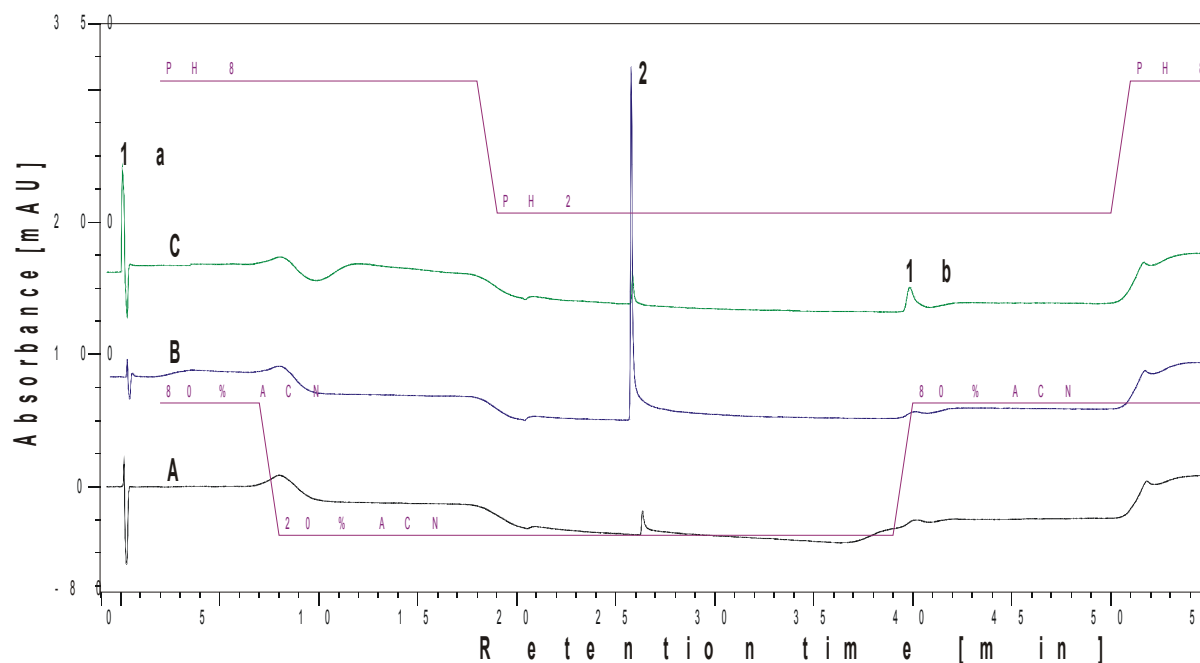


Figure 28: Elution of blank sample (A), imiquimod (B) and HSA (C); 20% ACN-step in gradient HSA passing the column (1a), elution of HSA-moiety (1b), imiquimod (2).

This resulting chromatographic method was further optimised to shorten the analysis time. Figure 29 shows the separation of a prepared mixed-standard of imiquimod and HSA through the optimised elution gradient (see. table 20), (1a), (1b) show the elution peaks of HSA and (2) the peak of imiquimod. Through the optimisation of all steps, the analysis time was reduced from 65 to 22 minutes.

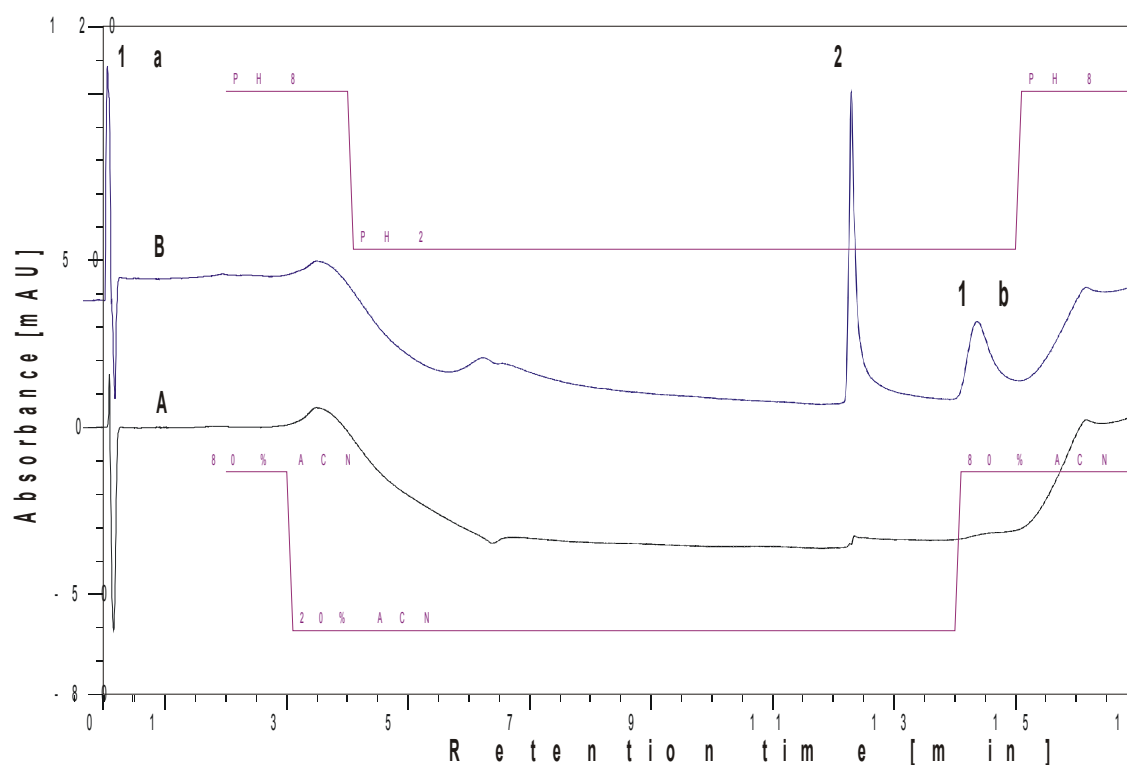


Figure 29: Chromatograms of blank sample (A) and mixed-standard (B), optimised gradient, HSA passing the column (1a), elution of HSA-moiety (1b), imiquimod (2).

4.4.2. Evaluation of the method for online-SPE of imiquimod

In order to create a method for the determination of imiquimod in ISF, a practicable sample preparation was implemented because of the high content of proteins of this human biofluid (1%, mainly HSA). The sample preparation included the precipitation of HSA through ACN-addition. Because of the fact, that only very small amounts of ISF were available, the investigation of the sample preparation had to be performed with a simulated matrix containing 1% HSA in NaCl 0.9M (physiological concentration).

Further, the established method including sample preparation was checked in its quality.

4.4.2.1. Sample preparation

Different amounts of ACN were added to simulated matrix and the resulting protein precipitation was investigated. Table 30 shows the observations for these preliminary tests illustrate, that the precipitation of HSA works best at high contents of ACN; it further was performed with 80% ACN.

Table 30: Results HSA-precipitation.

Precipitation tests of 1%HSA in physiological solution (0.9M NaCl)					
ACN-content [%]	80% ACN	70% ACN	60% ACN	50%ACN	40% ACN
Clouding	+++	+++	++	++	+
Pellet	+++	+++	++	++	+

+++) clearly observable ++) observable +) hardly observable

4.4.2.2. Method evaluation

Following experiments has been performed: Three different sample series have been prepared; A-, B- and C-samples (description below); each sample series was prepared three times. The obtained samples were analysed via the developed HPLC-method and measured as duplicate.

A-samples preparation: The simulated matrix was spiked with the respective standard (imiquimod 10-200ng/μl), subjected to the protein precipitation and finally analysed.

B-samples were prepared as follows: The simulated matrix without analyte was protein precipitated, after that spiked with the relevant standards in the concentrations 10-200ng/μl and analysed closing.

C-samples preparation: The “matrix” water was also subjected to the “protein precipitation”; the resulting solution was spiked with the imiquimod standards and further analysed.

Figure 30 shows the experimental scheme.

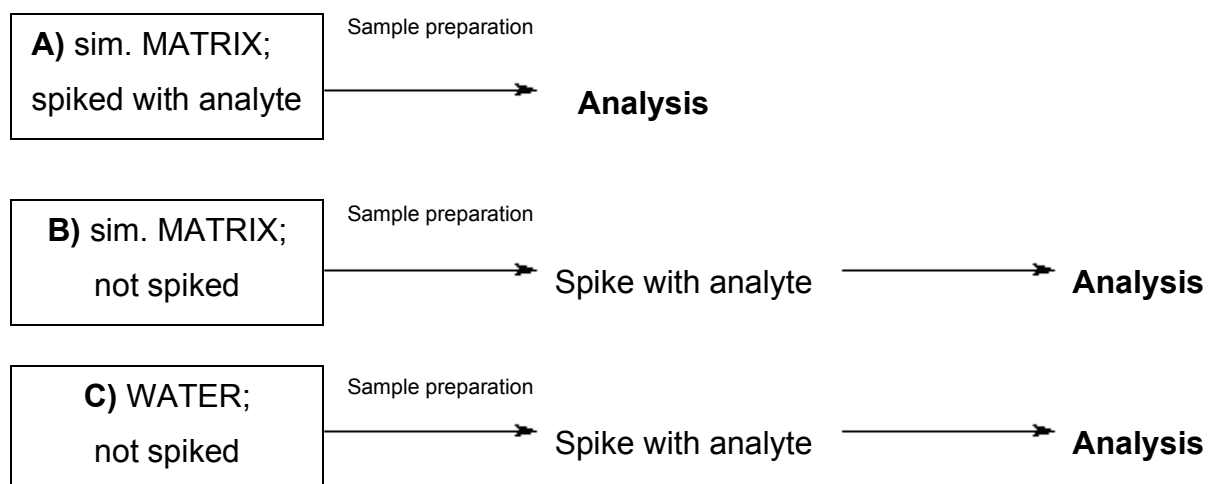


Figure 30: Experimental schema recovery-tests.

The values derived from the prepared A-samples analysis contain both: possibly errors through imiquimod losses while the sample extraction respective protein-precipitation and eventual errors through matrix effects of the analysis. B-samples values only include the potential errors through matrix effects of the analysis while the C-samples shouldn't include any failures. With the generated data the possible error-effects could be evaluated, this happened with the below mentioned equations 11-13.

$$ER = \frac{A}{B} * 100\% \quad \text{Equation 11}$$

ER... *Extraction recovery*

$$ME = \frac{B}{C} * 100\% \quad \text{Equation 12}$$

ME... *Matrix effect*

$$FDAREC. = \frac{A}{C} * 100\% \quad \text{Equation 13}$$

With the obtained values following aspects of the method were evaluated:

- Reproducibility of the HPLC-measurements
- Linearity of measuring range
- Reproducibility of the sample preparation
- Matrix effects and recovery

1.) The reproducibility of the measurements was investigated by double injection of the prepared samples and evaluation of the CVs of the derived values.

The results show that the reproducibility of the measurement is given with CVs from 1% to 7% for the duplicates whereas the higher values showed up very rarely.

2.) The linearity of the measurement range was evaluated through the generation of a calibration curve and its coefficient of determination R^2 , with this calibration curve the limit of quantification (LOQ) was determined.

Figure 31 shows the measured peak areas in dependence of the imiquimod concentration in the A-samples (matrix spiked with analyte) and as observable a well-fitting calibration curve can be generated through simple linear regression with a R^2 of 0.9966. This means, that the observed measurement range is linear.

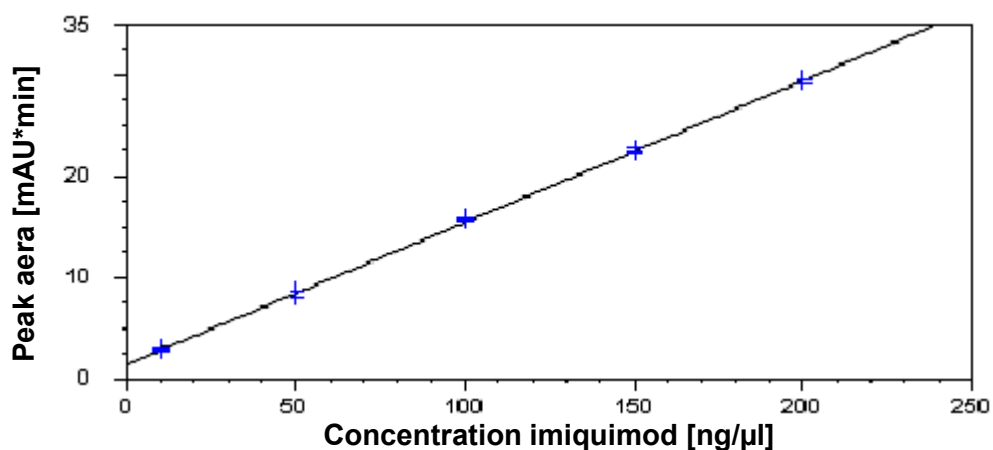


Figure 31: Calibration curve for A-samples.

The LOQ of this method (determined through the fivefold peak area of the blank response) was calculated to 6.4 ± 1.1 ng/μl

3.) To estimate the reproducibility of the sample preparation, each experimental series was prepared three times, the CV of the tests were evaluated.

The CV for the sample preparation shows with 2% to 8% good values; this applies for all, A, B and C-samples. Again, the higher values showed up rarely. This result demonstrates the reproducibility of the sample preparation very well.

4.) To identify possible interactions of the analyte with the matrix and/or effects of the protein precipitation the recovery of the imiquimod analysis was evaluated.

The results of the generated data show no clearly observable matrix effects or errors through sample preparation, the obtained values reach from 87-96% for the matrix effect and 83-105% for the extraction recovery. Therefore, the FDA-recovery is within 80-101%, which is a quite good value. There seems to be a trend to higher CV's for lower concentrations of imiquimod, but no clear statement can be made about this. The evaluated values are shown in figure 32 and also listed in table 31.

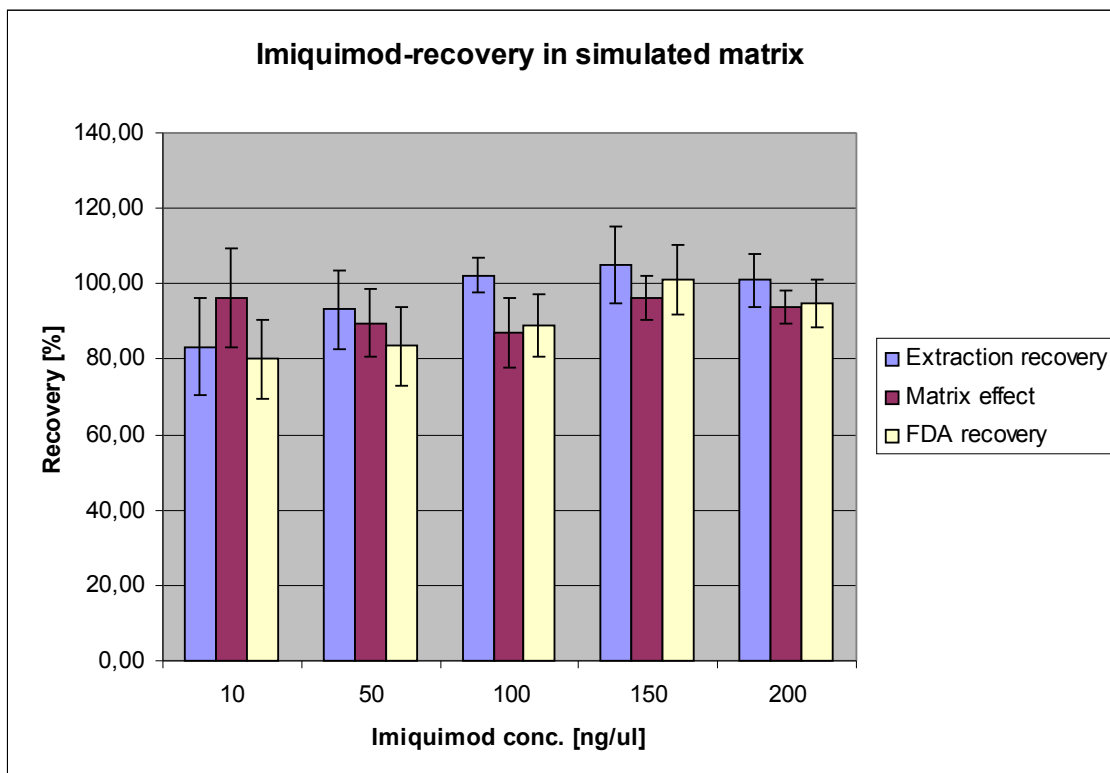


Figure 32: Recovery of imiquimod in simulated matrix.

Table 31: Recovery of imiquimod in simulated matrix.

Concentration Imiquimod	10ng/μl	50ng/μl	100ng/μl	150ng/μl	200ng/μl
ER [%]	83	93	102	105	101
CV [%]	12.8	10.4	4.8	10.2	7.1
ME [%]	96	89	87	96	94
CV [%]	13.1	9.0	9.4	6.0	4.4
FDA Rec. [%]	80	83	89	101	95
CV [%]	10.3	10.5	8.2	9.2	6.3

Summarised this method works very well; reproducibility is given for the measurement itself and for the execution of the sample preparation. The measurement range is linear and no clear matrix effects could be observed. Closing, the method had to be scrutinised with real human biofluid matrixes.

4.4.3. Online-SPE of imiquimod in human biofluids

To check the developed method in its performance, samples with real human biofluids had to be analysed.

For the generation of a calibration curve simulated matrix was spiked with imiquimod in concentrations from 10 to 200 ng/ μ l, after that subjected to the protein precipitation and further analysed (see 4.4.2.). These samples were measured three times. ISF and serum samples were prepared the same way, the respective matrix was spiked with imiquimod in concentrations of 50 and 150ng/ μ l, and then protein precipitated and analysed. These samples have been measured 5 times and the resulting values were checked in its accuracy.

All resulting samples were analysed with the established HPLC-method (see 4.4.1.).

Figure 33 shows the chromatograms for the online-SPE of imiquimod in the matrices simulated matrix, ISF and blood serum. As observable, the injection peaks are much higher for human biofluid samples, but this not precipitated protein passes the column while imiquimod is the only component loaded onto it, no further elution peak is detectable.

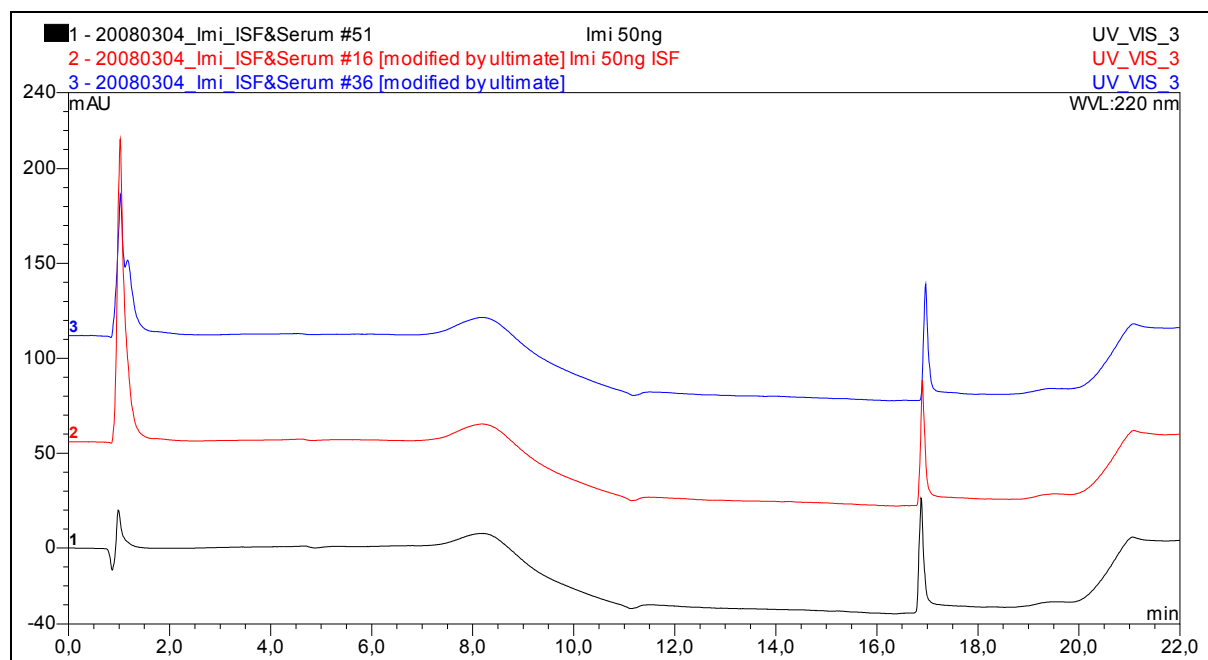


Figure 33: Comparison of online-SPE of imiquimod in different matrices; simulated matrix (A), ISF (B), blood serum (C).

Table 32 lists the obtained values for imiquimod in ISF and simulated matrix, they show good accuracy for all concentrations; also the CV is low. The values obtained from serum samples are also mentioned in table 32; they show fair accuracy and low CV. It seems that the recovery of imiquimod is a little bit higher in ISF; the values for serum samples consistently showed lower amounts of imiquimod. So it is possible, that some imiquimod is adsorbed on serum proteins and / or gets included in the precipitate. This effect naturally shows up much stronger for serum samples because of the higher amount of protein respectively precipitate.

Table 32: Accuracy imiquimod in different matrices.

Matrix	Accuracy 50 ng			Accuracy 150 ng		
	Sim. Matrix	ISF	Serum	Sim. Matrix	ISF	Serum
Conc. [ng/μl]	51	55	50	150	150	130
Accuracy [%]	102	110	100	100	100	87
CV [%]	3.1	3.8	3.5	3.5	2.0	1.5

Finally, the established method works very well for simulated matrix and ISF-samples, and no clear matrix effects were observable. The method should also be applicable for blood serum samples; the accuracy-values of imiquimod in serum are lower, but acceptable for many applications. However, an own calibration for blood serum samples is advisable.

This result shows that the investigated monoliths are well applicable in analytical problems in clinical research.

5. SUMMARY

ROMP-derived monolithic columns were functionalised via different techniques and at different conditions. Two functionalisation techniques were applied, *in-situ* grafting and *post-synthesis* grafting. The varied functionalisation conditions included changes of the functionalisation temperature and the content of NBE in the functionalisation mixture for *in-situ* grafted monoliths. The functionalisation conditions changed for *post-synthesis* grafted monoliths were the grafting temperature and the applied grafting catalyst. These functionalisation parameters led to different ion-exchange capacities; the chromatographic properties of these new separation media were characterised.

(1) The influence of the capacity on the separation performance was evaluated as well as the effect of the functionalisation parameter on the observed hydrophobicity of the functional separation material. These evaluations were performed for CX- and AX-monoliths.

(2) Further, the applicability of CX-monolithic separation media in clinical research was assessed with the online-SPE of imiquimod in human biofluids.

ad 1. All CX-monoliths showed good separation performance of peptides. There was no significant influence of the capacity on the separation performance observable; monoliths with higher ion-exchange capacities featured only a small increase in retention times as well as resolution.

For *in-situ* functionalised monoliths, the hydrophobicity of the CX-columns wasn't affected by the different functionalisation conditions. The applied functionalisation technique showed an influence on the hydrophobicity. *In-situ* grafted monoliths had a clearly observable hydrophobic character; *post-synthesis* grafting resulted in functional columns with decreased hydrophobicity.

The separation performance of most of the AX-monoliths was good, but some monoliths featured only poor oligonucleotide separation. Generally, there were big differences in the separation performance observable; the ion exchange capacity of the monoliths affected the separation performance in a positive way, but it turned out to be not the exclusive determining factor. Although the functionalisation parameters affect the capacity, they have a clear influence on the separation performance

beyond this. Not the monoliths with the highest capacities showed the best performance, but that which were grafted at higher temperatures. Changes of the grafting catalyst led to monoliths with higher capacities indeed, but this didn't increase the separation performance of the respective monoliths.

The hydrophobicity of the AX-columns was hardly evaluable because of the particulate poor separation; no clear influence of the applied functionalisation parameter on the hydrophobicity could be determined.

Ad 2. A method for the online-SPE of imiquimod in human biofluids such as ISF and blood serum was developed. It showed good recovery as well as accuracy.

All together, these results demonstrate the applicability of the ROMP-derived miniaturised functional monolithic separation media in clinical research very well.

6. References

1. Schrock, R. R. Ring-opening Polymerization, Brunelle, D.J., Ed.; Hanser: Munich

- 1993.
2. Sinner, F. M.; Buchmeiser, M. R. *Angew Chem* 2000; 112: 1491-94.
 3. Sinner, F. M.; Buchmeiser, M. R. *Macromolecules* 2000, 33, 5777-86.
 4. Mayr, B.; Hölzl, G.; Eder, K.; Buchmeiser, M. R.; Huber, C. G. *Anal Chem* 2002; 74: 6080-87.
 5. Sinner, F.; Gatschelhofer, C. *J Chrom A* 2008; in press.
 6. Ettre, L. S.; *Pure & Appl Chem* 1993; 65: 819-72.
 7. Strancar, A.; Podgornik, A.; Barut, M.; Necina, R. *Adv Biochem Eng Biotechnol* 2002; 76: 49-85.
 8. Leinweber, Felix, Tallarek, Ulrich *J Chromatogr A* 2003; 1006: 207-28.
 9. Szepesi, G. *HPLC in Pharmaceutical Analysis*, 1990, Chapter 2.
 10. Snyder, D. R.; Kirkland, J. J. *Introduction to Modern Liquid Chromatography*, Wiley: New-York, 1979.
 11. Dekker, M. *Packing and Stationary Phases in Chromatographic Techniques*, New-York, 1990.
 12. Afeyan, N. B.; Fulton, S. P.; Regnier, F. E. *J Chromatogr* 1991; 544: 267-79.
 13. Tennikova, T. B.; Bleha, M.; Svec, F.; Almazova, T.V.; Belenkii, B. G. *J Chromatogr A* 1991; 555: 97-107.
 14. Gerstner, J. A.; Hamilton, R.; Kramer, S. M. *J Chromatogr A* 1992; 596: 173.
 15. Kennedy, J. F.; Paterson, M. *Polymer Int* 1993; 32: 71.
 16. Yang, Y.; Velayudhan, A.; Ladish, C. M.; Ladish, M. R. *J Chromatogr A* 1992; 598: 169.
 17. Vlakh, E. G.; Tennikova, T. B. *J Sep Sci* 2007; 30: 2801.
 18. Svec, F.; Frechet, J. M. J. *Ind Eng Chem Res* 1999; 38:34-48.
 19. Svec, F.; Peters, E.; Sykora, D.; Yu, C.; Frechet, J. M. J. *J High Resolut Chromatogr* 2000; 23:3-18.
 20. Buchmeiser, M. R.; *Macromol Rapid Commun* 2001; 22:1081-94.
 21. Buchmeiser, M. R.; *Polymer* 2007; 48:2187-98.
 22. Svec, F. Tennikova, T. B.; Deyl, Z.; editors. *Monolithic materials: Preparation, properties and applications*: Elsevier; 2003.
- Kubin, M.; Spacek, P.; Chromecek, R. *Collect Czech Chem Commun* 1967; 32: 3881-7.
23. 3881-7.
 24. Ross, W. D.; Jefferson, R. T. *J Chromatogr Sci* 1970; 8:386-9.
 25. Hileman, F. D.; Sievers, R. E.; Hess, G. G.; Ross, W. D. *Anal Chem* 1973; 45: 1126-30.
 26. Hjerten, S.; Liao, J-L.; Zhang, R. *J Chromatogr A* 1989; 473:273-5.
 27. Hjerten, S.; Li, Y-M.; Liao, J-L.; Mohammad, J.; Nakazato, K.; Petterson, G. *Nature* 1992; 356:810-1.
 28. Hjerten, S.; Nakazato, K.; Mohammed, J.; Eaker D. *Chromatographia* 1993; 37: 287-94.
 29. Belenkii, B. G.; Podkladenko, A. M.; Kurenbin, O. I.; Mal'tsev, V. G.; Nasledov, D. G.; Trushin, S. A. *J Chromatogr A* 1993; 645: 1-15.
 30. Mal'tsev, V. G.; Nasledov, D. G.; Trushin, S. A.; Tennikova, T. B.; Vinogradova,

- S.V.; Volokitina, I. N. et al. *J Resolut Chromatogr* 1990; 13:185-9.
31. Tennikova, T. B.; Belenkii, B. G.; Svec, F. *J Liq Chrom Rel technol* 1990; 13:63-70.
 32. Rodrigues, A. E.; Mata, V. G.; Zabka, M.; Pais, L. Flow and mass transfer. In: Svec, F.; Tennikova, T. B.; Deyl, Z.; editors. *Monolithic materials: preparation, properties and applications. J Chromatogr Libr, Vol. 67.* Amsterdam: Elsevier; 2003.
 33. Nakanishi, K.; Minakuchi, H.; Soga, N.; Tanaka, N. *J Sol-Gel Sci Technol* 8:547; 1997.
 34. Minakuchi, H.; Nakanishi, K.; Soga, N.; Ishizuka, N.; Tanaka, N. *J Chromatogr A*; 762:135; 1997.
 35. Ishizuka, N.; Minakuchi, H.; Nakanishi, K.; Hirao, K.; Tanaka, N. *Colloids Surf A*; 187-188, 273; 2001.
 36. Nawrocki, J.; Dunlap, C.; Li, J.; Zhao, J.; McNeff, C.V.; McCormick, A.; Carr, P.W. *J Chromatogr A* 2004; 1028: 31.
 37. Taguchi, A.; Smatt, J. H.; Linden, M. *Adv Mater* 2003; 15: 1209.
 38. Liang, C.; Dai, S.; Guichon, G. *Anal Chem* 2003; 75: 4904.
 39. Guiochon, G.; *J Chromatogr A* 2007; 1168: 101-168.
 40. Viklund, C.; Ponten, E.; Glad, B.; Irgum, K.; Hörstedt, P.; Svec, F. *Chem mater* 1997; 9:463-71.
 41. Safrany, A.; Beiler, B.; Laszlo, K.; Svec, F. *Polymer* 2005; 46: 2862-71.
 42. Bandari, R.; Knolle, W.; Prager-Duschke, A.; Buchmeiser, M. R. *J Chrom A* 2008; in press.
 43. Hosoya, K.; Hira, N.; Yamamoto, K.; Nishimura, M.; Tanaka, N. *Anal Chem* 2006; 78: 5729-35.
 44. Tsujioka, N.; Hira, N.; Aoki, S.; Tanaka, N.; Hosoya, K. *Macromolecules* 2005; 38: 9901-3.
 45. Nguyen, A. M.; Irgum, K. *Chem Mater* 2006; 18: 6308-15.
 46. Stelzer, F. *JMS-Pure Appl Chem*; 1996; A33: 941.
 47. Grubbs, G. H. *Comprehensive Organometallic Chemistry.*; Wilkinson, G.; Stone, F. G.; A. Abel, E.; Eds.; Pergamon: Oxford, 1982.
 48. O'Dell, R.; McConville, D. H.; Hofmeister, G. E.; Schrock, R. R. *J Am Chem Soc* 1994; 116: 3414-23.
 49. Schimetta, M.; Stelzer, F. *Macromolecules* 1994; 27: 3769-72.
 50. Dall'Asta, G.; Motroni, G. *Eur Poly J* 1971; 7: 707-16.
 51. Calderon, N.; Ofstead, E. A.; Judy, W. A. *Angew Chem* 1976; 88: 433-42.
 52. Chauvin, Y.; Herisson, J. L. *Macromol Chem* 1970; 141: 161.
 53. Rappe, A. K.; Goddard, W. A. *J Am Chem Soc* 1986; 101: 5114.
 54. Ebdon, J. R.; Eastmond, G. C.; *New Methods of polymer synthesis*, Chapman & Hall: London, Glasgow, Weinheim, New-York, Tokyo, Melbourne, Madras, 1995.
 55. Weck, M.; Schwab, P.; Grubbs, R. H. *Macromolecules* 1996; 29: 1789-93.
 56. Peters, E. C.; Svec, F.; Frechet, J. M. J. *Adv Mater* 1999; 11:1169-81.
 57. Guyot, A.; Bartholin, M. *Prog Polym Sci* 1982; 8: 277-332.
 58. Wulff, G. *Angew Chem* 1995; 107: 1958-79.
 59. Hahn, R.; Podgornik, A.; Merhar, M.; Schallaun, E.; Jungbauer, A. *Anal Chem* 2001; 73: 5126-32.

60. Svec, F.; Frechet, J. M. J. *J Chrom A* 1995; 702: 89-95.
61. Jain, S. R.; Borowska, E.; Davidsson, R.; Tudorache, M.; Ponten, E.; Emneus, J. *Biosens Bioelectr* 2004; 19:975-803.
62. Gusev, I.; Huang, X.; Horvath, C. *J Chromatogr A* 1999; 855: 273-90.
63. Huang, X.; Zhang, S.; Schultz, G. A.; Henion, J. *Anal Chem* 2003; 75: 5328-35.
64. Rohr, T.; Hilder, E. F.; Donovan, J. J.; Svec, F.; Frechet, J. M. J. *Macromolecules* 2003; 36: 1677-84.
65. Hilder, E. F.; Svec, F.; Frechet, J. M. J. *Anal Chem* 2004; 76: 3887-92.
66. Meyer, U.; Svec, F.; Frechet, J. M. J.; Hawker, C. J.; Irgum, K. *Macromolecules* 2000; 33:7769-75
67. Buchmeiser, M. R.; Atzl, N.; Bonn, G. K. *J Am Chem Soc* 1997; 119: 9166-74.
68. Sinner, F.; Buchmeiser, M. R.; Tessadri, R.; Mupa, M.; Wurst, K.; Bonn, G. K. *J Am Chem Soc* 1998; 120: 2790-7.
69. Buchmeiser, M. R.; Tessadri, R.; Seeber, G.; Bonn, G. K. *Anal Chem* 1998; 70: 2130-6.
70. Buchmeiser, M. R.; Bonn, G. K. *Am Lab* 1998; 11: 16-9.
71. Buchmeiser, M. R.; Mupa, M.; Seeber, G.; Bonn, G. K. *Chem Mater* 1999; 11: 1533-40.
72. Buchmeiser, M. R.; Sinner, F.; Mupa, M.; Wurst, K. *Macromolecules* 2000; 33:32-9.
73. Matyjaszewski, K. *Macromolecules* 1993; 26: 1787-8.
74. Szwarc, M. *J Polym Sci A Polym Chem* 1998; 36: 9-15.
75. Mayr, B.; Buchmeiser, M. R. *J Chromatogr A* 2001; 907: 73-80.
76. Gatschelhofer, C.; Magnes, C.; Pieber, T. R.; Buchmeiser, M. R.; Sinner, F. *J Chromatogr A* 2005; 1090: 81-89
77. Lubbad, S.; Buchmeiser, M. R. *Macromol Rapid Commun* 2003; 24: 580-4.
78. Pickl, K. E.; Magnes, C.; Bodenlenz, M.; Pieber, T. R.; Sinner, F. *J Chromatogr B* 2007; 850: 432-439.
79. Gupta, A. K.; Davey, V.; McPhail, H. *J Cutan Med Surg* 2005; 5: 209-14.
80. Harrison, L. I.; Skinner, S. L.; Marbury, T. C.; Owens, M. L.; Kurup, S.; McKane, S.; Greene, R. J. *Arch Dermatol Res* 2004; 296: 6-11.
81. Soria, I.; Myhre, P.; Horton, V.; Ellefsun, P.; McCarville, S.; Schmitt, K.; Owens, M. *Int J Clin Pharmacol Ther* 2000; 38: 476-81.

List of Publications and Posters

Publications

1. Christina Gatschelhofer, Agnes Mautner, Franz Reiter, Thomas R. Pieber, Michael R. Buchmeiser, Frank M. Sinner:
Ring-opening metathesis polymerization for the preparation of norbornene-based weak cation-exchange monolithic capillary columns.
J. Chromatography A, 2008 in press.

Posters

1. Christina Gatschelhofer, Agnes Mautner, Franz Reiter, Michael R. Buchmeiser, Andreas Zimmer, Karin Wernig, Thomas R. Pieber, Frank M. Sinner:
Development of Capillary-Scale Monolithic Supports for On-Line Sample Pre-treatment in Nanomedical Research
2nd International Graz Workshop for Pharmaceutical Engineering Science, 15. 05. - 16. 05. 2008, Graz, Austria
2. Agnes Mautner, Christina Gatschelhofer, Franz Reiter, Michael R. Buchmeiser, Thomas R. Pieber, Frank M. Sinner:
Functionalization of ROMP-derived monolithic capillary columns and their chromatographic properties
3rd Monolith Summer School and Symposium, 30.05. - 04. 06. 2008, Portoroz, Slovenia
3. Christina Gatschelhofer, Agnes Mautner, Franz Reiter, Michael R. Buchmeiser, Andreas Zimmer, Karin Wernig, Thomas R. Pieber, Frank M. Sinner:
Development of Capillary-Scale Monolithic Supports for On-Line Sample Pre-treatment in Nanomedical Research
9th Symposium on Instrumental Analysis, 29. 06. - 02. 07. 2008, Pécs, Hungary

Index of figures

Figure 1: Chromatographic parameters of a chromatogram [6].	10
Figure 2: Morphology of separation media [8].	14
Figure 3: Formation of unsaturated linear polymers from cycloolefines as side-reaction [46].	20
Figure 4: Chauvin reaction-mechanism of ROMP.	21
Figure 5: Difference between Fischer- and Schrock-carbenes.	21
Figure 6: General reaction scheme of ring-opening metathesis polymerisation.	22
Figure 7: Possible regular structures of 2,3 – di-substituted norbornadiens.	23
Figure 8: Reaction schema for preparation of a ROMP-derived RP-monolith.	25
Figure 9: Reaction schema for preparation of an in-situ grafted ROMP-derived monolith.	26
Figure 10: Separation performance depending on the buffer concentration: 1mM buffer (A), 5mM (B), 10mM (C).	44
Figure 11: Peptide separation of M1 at 40% ACN.	45
Figure 12: Peptide separation at 40% of M1 ACN (A) compared to M2 (B).	47
Figure 13: Peptide separation of M2 at 40% ACN (A) compared to M3 (B).	49
Figure 14: Comparison of tR at 40% ACN of M1 – M3.	51
Figure 15: Assessment hydrophobicity of M2; 40% ACN (A), 30% ACN (B).	52
Figure 16: Assessment hydrophobicity of M3; 40% ACN (A), 30% ACN (B).	53
Figure 17: Separation performance at 20mM (A) and 5mM buffer concentration (B).	55
Figure 18: Elution-gradients; Gradient slope NaCl 100mM/min (A), 50mM/min (B), 15mM/min (C).	56
Figure 19: Separation performance at 15% ACN for M4 (A) and M5 (B).	58
Figure 20: Separation performance of M6 (A) and M7 (B) at 30% ACN.	59
Figure 21: Separation performance of M8 (A) and M9 (B) at 30% ACN.	60
Figure 22: Separation performance of M7 (A) compared to M9 (B) at 30% ACN.	60
Figure 23: Chromatograms for M5 at different ACN-contents; 30% ACN (A); 25% ACN (B); 20% ACN (C); 15% ACN (D); 10% ACN (E).	63
Figure 24: Separation performance for M7 at decreasing ACN-contents; 30% ACN (A); 25% ACN (B); 20% ACN (C); 15% ACN (D); 10% ACN (E).	63
Figure 25: Separation performance for M9 at decreasing ACN-contents; 30% ACN (A); 25% ACN (B); 20% ACN (C); 15% ACN (D); 10% ACN (E).	64
Figure 26: Structure of imiquimod.	65
Figure 27: Elution of imiquimod (A) and HSA (B) through pH-step 8-2 at 80% ACN.	68
Figure 28: Elution of blank sample (A), imiquimod (B) and HSA (C); 20% ACN-step in gradient.	69
Figure 29: Chromatograms of blank sample (A) and mixed-standard (B), optimised gradient, HSA passing the column (1a), elution of HSA-moiety (1b), imiquimod (2).	70
Figure 30: Experimental schema recovery-tests.	72
Figure 31: Calibration curve for A-samples.	74
Figure 32: Recovery of imiquimod in simulated matrix.	75
Figure 33: Comparison of online-SPE of imiquimod in different matrices; simulated matrix (A), ISF (B), blood serum (C).	76

Index of tables

Table 1: Common packed column types [9].....	15
Table 2: Overview of the properties of separation material in HPLC.....	16
Table 3: Commercial available monolithic products in chromatography [17].....	18
Table 4: Overview provided monoliths CX.	27
Table 5: Overview provided monoliths AX.	27
Table 6: Materials.....	28
Table 7: Equipment.....	28
Table 8: Chemicals for the preparation of the mobile phase.....	28
Table 9: Chemicals for standards.....	28
Table 10: Used synthetic peptides.....	30
Table 11: Composition of the mixed standard.	30
Table 12: Contents of the mobile phases for CX-monoliths.....	31
Table 13: Solvent gradient for CX separations; 30% ACN isocratic.....	32
Table 14: Contents of the mobile phases for AX-separations.....	33
Table 15: Solvent gradient for AX-separations at 30% ACN isocratic.....	33
Table 16: Solvent gradient for RP-measurement.....	35
Table 17: HSA-precipitation tests of simulated matrix.	36
Table 18: A-samples composition – simulated matrix spiked.....	37
Table 19: B-samples composition – simulated matrix not spiked.....	37
Table 20: C-samples composition - water not spiked.....	38
Table 21: Contents of the mobile phases for imiquimod/HSA behaviour-studies.	39
Table 22: Elution gradient imiquimod/HSA-investigations.....	39
Table 23: Optimised eluent-gradient for online-SPE of imiquimod.....	40
Table 24: Charge and hydrophobicity index used synthetic peptides.....	42
Table 25: Retention times (tR), peak widths (w1/2), peak symmetry (S) and resolution (R) for M1 at 40% ACN.	46
Table 26: Retention times (tR), peak widths (w1/2), peak symmetry (S) and resolution (R) for M2 at 40% ACN.	48
Table 27: Retention times (tR), peak widths (w1/2), peak symmetry (S) and resolution (R) for M3 at 40% ACN.	50
Table 28: Separation parameter of M7 compared to M9 at 30% ACN.....	61
Table 29: tR – increase (pT12) of M7 and M9 at ACN-content – decrease.....	64
Table 30: Results HSA-precipitation.....	71
Table 31: Recovery of imiquimod in simulated matrix.....	75
Table 32: Accuracy imiquimod in different matrices.....	77